Molecular Biology of the Cell
Vol. 12, 1239–1255, May 2001

Isolation and Characterization of Effector-Loop Mutants of *CDC42* in Yeast

Amy S. Gladfelter, John J. Moskow, Trevin R. Zyla, and Daniel J. Lew*

Department of Pharmacology and Cancer Biology, Duke University Medical Center, Durham, North Carolina 27710

Submitted September 19, 2000; Revised December 22, 2000; Accepted February 20, 2001
Monitoring Editor: Tim Stearns

The highly conserved small GTPase Cdc42p is a key regulator of cell polarity and cytoskeletal organization in eukaryotic cells. Multiple effectors of Cdc42p have been identified, although it is unclear how their activities are coordinated to produce particular cell behaviors. One strategy used to address the contributions made by different effector pathways downstream of small GTPases has been the use of "effector-loop" mutants of the GTPase that selectively impair only a subset of effector pathways. We now report the generation and preliminary characterization of a set of effector-loop mutants of *Saccharomyces cerevisiae CDC42*. These mutants define genetically separable pathways influencing actin or septin organization. We have characterized the phenotypic defects of these mutants and the binding defects of the encoded proteins to known yeast Cdc42p effectors in vitro. The results suggest that these effectors cannot account for the observed phenotypes, and therefore that unknown effectors exist that affect both actin and septin organization. The availability of partial function alleles of *CDC42* in a genetically tractable system serves as a useful starting point for genetic approaches to identify such novel effectors.

INTRODUCTION

The establishment and regulation of cell polarity are critical for cell shape, for cell motility and migration, and for directional cell–cell communication. Although the detailed forms and consequences of polarization vary widely depending on the cell type and the biological context, the underlying molecular machinery used to establish cell polarity appears to be remarkably well conserved among eukaryotes. In particular, the small GTPase Cdc42p, originally identified through its role in polarization of yeast cells during bud formation (Adams *et al.*, 1990), plays a widespread role in polarity establishment and cytoskeletal regulation throughout eukaryotes (Hall, 1998; Johnson, 1999). Cdc42p can stimulate actin polymerization and reorganization (Li *et al.*, 1995; Zigmond *et al.*, 1998; Bi and Zigmond, 1999; Rohatgi *et al.*, 1999), affect vesicle trafficking (Brown *et al.*, 1998; Kroschewski *et al.*, 1999; Garrett *et al.*, 2000), and influence transcriptional regulation (Coso *et al.*, 1995; Minden *et al.*, 1995; Simon *et al.*, 1995; Zhao *et al.*, 1995). These functions are thought to be mediated by numerous effectors (proteins that are regulated through their specific interaction with GTP-bound Cdc42p), and intensive efforts are underway to identify effectors and to elucidate how Cdc42p coordinates their actions to promote appropriate effects.

Several potential Cdc42p effectors have been identified through a variety of interaction-cloning strategies (Manser *et al.*, 1993, 1994), and recognition of a conserved Cdc42/Rac-interactive-binding (CRIB) domain (Burbelo *et al.*, 1995) has allowed the discovery of further effectors by virtue of sequence homology (Brown *et al.*, 1997; Chen *et al.*, 1997; Martin *et al.*, 1997; Pirone *et al.*, 2000). However, there is considerable controversy regarding the role of particular effectors in specific responses (Lamarche *et al.*, 1996; Sells *et al.*, 1997), and it is not clear whether the majority of effectors have been identified or whether many yet remain to be discovered. Perhaps surprisingly, genetic approaches in yeast have thus far contributed little to the identification of Cdc42p effectors, possibly because until recently very few mutant *cdc42* alleles were available for analysis.

One approach that has enjoyed remarkable success in the analysis of pathways downstream of Ras-related GTPases is the use of mutants that alter residues in the "effector loop" of the protein, which is thought to enable interacting proteins to recognize the "activated" GTP-bound conformation (Wittinghofer and Nassar, 1996). In many instances, effector-loop mutations appear to selectively disrupt the interaction of GTP-bound Ras relatives with only a subset of their effectors (Nobes and Hall, 1995; White *et al.*, 1995; Joneson *et al.*, 1996a,b; Khosravi-Far *et al.*, 1996; Lamarche *et al.*, 1996; White *et al.*, 1996; Joneson and Bar-Sagi, 1997; Sahai *et al.*, 1998; Owen *et al.*, 2000). When effector-loop mutant alleles are introduced into cells, phenotypic deficits in specific biological outputs can be correlated with biochemical deficits in binding to particular effectors. Although this approach has been applied to ask whether known effectors are likely to

* Corresponding author. E-mail address: daniel.lew@duke.edu.

Table 1. Yeast strains used in this study[a]

Strain	Genotype
DLY1	**a** *bar1*
DLY5	**a**/α
DLY680	α *cdc42-1*
DLY3067	**a** *bar1 cdc42::LEU2::GAL1p-CDC42*
DLY3496	**a** *bar1 leu2::GAL1p-CDC42::LEU2 cdc42^{N39A}*
DLY3497	**a** *bar1 leu2::GAL1p-CDC42::LEU2 cdc42^{V36A}*
DLY3500	**a** *bar1 leu2::GAL1p-CDC42::LEU2 cdc42^{V36T}*
DLY3509	**a** *bar1 cdc42::LEU2::GAL1p-CDC42 his2::cdc42^{D38I}::HIS2*
DLY3511	**a** *bar1 cdc42::LEU2::GAL1p-CDC42 his2::cdc42^{T35A}::HIS2*
DLY3513	**a** *bar1 cdc42::LEU2::GAL1p-CDC42 his2::cdc42^{Y40K}::HIS2*
DLY3515	**a** *bar1 cdc42::LEU2::GAL1p-CDC42 his2::cdc42^{D38A}::HIS2*
DLY3517	**a** *bar1 cdc42::LEU2::GAL1p-CDC42 his2::cdc42^{F37G}::HIS2*
DLY3519	**a** *bar1 cdc42::LEU2::GAL1p-CDC42 his2::cdc42^{Y40C}::HIS2*
DLY3525	α *bar1 cdc42::LEU2::GAL1p-CDC42 his2::cdc42^{Y40C}::HIS2*
DLY3540	α *bar1 his2::cdc42^{Y40K}::HIS2 cdc42-6*
DLY3541	α *bar1 his2::cdc42^{D38A}::HIS2 cdc42-6*
DLY3553	α *bar1 leu2::GAL1p-CDC42::LEU2 cdc42^{V36T}*
DLY3554	α *bar1 leu2::GAL1p-CDC42::LEU2 cdc42^{V36A}*
DLY3556	α *bar1 leu2::GAL1p-CDC42::LEU2 cdc42^{N39A}*
DLY3571[b]	**a**/α *bar1/bar1 cdc42::LEU2::GAL1p-CDC42/cdc42::LEU2::GAL1p-CDC42 his2::cdc42^{F37G}::HIS2/his2::cdc42^{F37G}::HIS2*
DLY3572[b]	**a**/α *bar1/bar1 cdc42::LEU2::GAL1p-CDC42/cdc42::LEU2::GAL1p-CDC42 his2::cdc42^{Y40K}::HIS2/his2::cdc42^{Y40K}::HIS2*
DLY3579	α *bar1 his2::cdc42^{F37G}::HIS2 cdc42-6*
DLY3804	α *bar1 his2::cdc42^{D38I}::HIS2 cdc42-6*
DLY3809	α *bar1 cdc42::LEU2::GAL1p-CDC42 his2::cdc42^{T35A}::HIS2*
DLY3880	α *bar1 cdc42::LEU2::GAL1p-CDC42 his2::cdc42^{F37Y}::HIS2*
DLY3881	α *bar1 cdc42::LEU2::GAL1p-CDC42 his2::cdc42^{F37Y}::HIS2*
DLY3891	**a**/α *bar1/bar1 leu2::GAL1p-CDC42::LEU2/leu2 cdc42::LEU2::GAL1p-CDC42/cdc42^{V36T}his2::cdc42^{F37G}::HIS2/his2*
DLY3895	**a**/α *bar1/bar1 leu2::GAL1p-CDC42::LEU2/leu2 cdc42::LEU2::GAL1p-CDC42/cdc42^{V36T}his2::cdc42^{Y40K}::HIS2/his2*
DLY3923	**a**/α *bar1/bar1 leu2::GAL1p-CDC42::LEU/leu2::GAL1p-CDC42::LEU2 cdc42^{V36A}/cdc42^{V36A}*
DLY3924	**a**/α *bar1/bar1 leu2::GAL1p-CDC42::LEU/leu2::GAL1p-CDC42::LEU2 cdc42^{V36T}/cdc42^{V36T}*
DLY4756	**a**/α *bar1/bar1 cdc42::LEU2::GAL1p-CDC42/cdc42::LEU2::GAL1p-CDC42 his2::cdc42^{F37Y}::HIS2/his2::cdc42^{F37Y}::HIS2*
DLY4757	**a**/α *bar1/bar1 leu2::GAL1p-CDC42::LEU2/leu2::GAL1p-CDC42::LEU2 cdc42^{N39A}/cdc42^{N39A}*
MOSY0090	**a** *bar1 leu2::GAL1p-CDC42::LEU2 cdc42::URA3*
MOSY0121	α *bar1 cdc42-6*

[a] All strains are in the BF264-15Du (Richardson *et al.*, 1989) background (*ade1 his2 leu2-3, 112 trp1-1 ura3*Δ*ns*).
[b] DLY3571 and DLY3572 were generated by *HO*-induced diploidization of DLY3517 and DLY3513, respectively.

participate in particular pathways, it has not yet contributed to the search for novel effectors.

We reasoned that introduction of effector-loop mutants of *CDC42* into the genetically tractable yeast system should provide strains containing partial function *cdc42* alleles that could serve as a productive starting point for genetic approaches to identify novel Cdc42p effectors and to assign roles for known effectors in particular pathways. Here we report the generation and phenotypic and biochemical characterization of 10 effector-loop mutants. The results suggest that as-yet-unknown effectors exist in yeast, and that some "effectors" may operate upstream of Cdc42p as well as downstream of Cdc42p.

MATERIALS AND METHODS

Strains, Plasmids, and PCR Manipulations

Standard media and methods were used for plasmid manipulations (Ausubel *et al.*, 1995) and yeast genetic manipulations (Guthrie and Fink, 1991). The *Saccharomyces cerevisiae* strains used in this study are listed in Table 1, plasmids are listed in Table 2, and oligonucleotides are listed in Table 3.

The *CDC42* effector-loop mutants were constructed using the ExSite polymerase chain reaction (PCR)-based site-directed mutagenesis kit (Stratagene, La Jolla, CA). For each mutation, PCR was performed using the mutagenic and cdc-11 oligonucleotides (Table 3) with pDLB643 as a template. This plasmid contains the *CDC42* promoter and coding region (from 366 bp upstream of the start codon to 30 bp downstream of the stop codon) fused to *TDH3* transcription terminator sequences in a pCR2.1 (Invitrogen, Carlsbad, CA) backbone (Moskow *et al.*, 2000).

Using the above-mentioned mutants as template, the *CDC42* and *TDH3* sequences were amplified by PCR with the oligonucleotides DJL42-3 and DJL42-6 (Table 3) and introduced into pDLB644 (Moskow *et al.*, 2000) by gap repair, generating plasmids for expression of *cdc42* alleles in yeast. Mutants were sequenced to confirm the presence of the desired mutation and the absence of any other mutations. These plasmids contain a pRS316 (Sikorski and Hieter, 1989) backbone (low-copy *URA3*), and parallel sets of plasmids was generated by subcloning the 2.1-kb *Bam*HI/*Xho*I fragments containing *cdc42* alleles into the corresponding sites in pRS314 (low-copy *TRP1*), pRS424 (high-copy *TRP1*), and pRS426 (high-copy *URA3*) vectors (Sikorski and Hieter, 1989).

Table 2. Plasmids used in this study

Plasmid	Vector	Insert	Source
pDLB678	2 μm *URA3*	*BEM1*	Bender and Pringle, 1991
pDLB722	2 μm *URA3*	*CLA4*	Erfei Bi
pDLB723	2 μm *URA3*	*STE20*	Erfei Bi
pDLB935	YEp24	*CDC24*	John Moskow[a]
pDLB1025	pUNI10[b]	*CLA4* CRIB	This study
pDLB1026	pUNI10[b]	*GIC1* CRIB	This study
pDLB1027	pUNI10[b]	*GIC2* CRIB	This study
pDLB1034	pUNI10[b]	$cdc42^{Q61L}$	This study
pDLB1035	pUNI10[b]	$cdc42^{D57Y}$	This study
pDLB1126	pHB2-GST[b]	*CLA4* CRIB	This study
pDLB1127	pHB2-GST[b]	*GIC1* CRIB	This study
pDLB1128	pHB2-GST[b]	*GIC2* CRIB	This study
pDLB1159	pUNI10[b]	$cdc42^{V36T,Q61L}$	This study
pDLB1160	pUNI10[b]	$cdc42^{V36A,Q61L}$	This study
pDLB1161	pUNI10[b]	$cdc42^{F37G,Q61L}$	This study
pDLB1234	pHB1-myc3[b]	$cdc42^{D57Y}$	This study
pDLB1238	pHB1-myc3[b]	$cdc42^{Q61L}$	This study
pDLB1239	pHB1-myc3[b]	$cdc42^{T35A,Q61L}$	This study
pDLB1240	pHB1-myc3[b]	$cdc42^{V36A,Q61L}$	This study
pDLB1241	pHB1-myc3[b]	$cdc42^{V36T,Q61L}$	This study
pDLB1242	pHB1-myc3[b]	$cdc42^{Y40C,Q61L}$	This study
pDLB1243	pHB1-myc3[b]	$cdc42^{Y40K,Q61L}$	This study
pDLB1274	pUNI10[b]	*BEM1*	This study
pDLB1275	pUNI10[b]	$cdc42^{T35A,Q61L}$	This study
pDLB1277	pUNI10[b]	$cdc42^{Y40C,Q61L}$	This study
pDLB1278	pUNI10[b]	$cdc42^{F37Y,Q61L}$	This study
pDLB1279	pUNI10[b]	$cdc42^{D38A,Q61L}$	This study
pDLB1280	pUNI10[b]	$cdc42^{N39A,Q61L}$	This study
pDLB1282	pHB1-myc3[b]	$cdc42^{F37G,Q61L}$	This study
pDLB1283	pHB1-myc3[b]	$cdc42^{F37Y,Q61L}$	This study
pDLB1284	pHB1-myc3[b]	$cdc42^{D38A,Q61L}$	This study
pDLB1285	pHB1-myc3[b]	$cdc42^{D38I,Q61L}$	This study
pDLB1286	pHB1-myc3[b]	$cdc42^{N39A,Q61L}$	This study
pDLB1305	pHB2-GST[b]	*BEM1*	This study
pDLB1307	pUNI10[b]	$cdc42^{Y40K,Q61L}$	This study
pDLB1308	2 μm *URA3*	*HA-BNI1*	Mark Longtine
pDLB1309	pHB2-GST[b]	$cdc42^{Q61L}$	This study
pDLB1311	pHB2-GST[b]	$cdc42^{D57Y}$	This study
pDLB1313	pHB2-GST[b]	$cdc42^{T35A,Q61L}$	This study
pDLB1314	pHB2-GST[b]	$cdc42^{V36A,Q61L}$	This study
pDLB1315	pHB2-GST[b]	$cdc42^{V36T,Q61L}$	This study
pDLB1316	pHB2-GST[b]	$cdc42^{F37G,Q61L}$	This study
pDLB1317	pHB2-GST[b]	$cdc42^{F37Y,Q61L}$	This study
pDLB1318	pHB2-GST[b]	$cdc42^{D38A,Q61L}$	This study
pDLB1319	pHB2-GST[b]	$cdc42^{D38I,Q61L}$	This study
pDLB1320	pHB2-GST[b]	$cdc42^{N39A,Q61L}$	This study
pDLB1321	pHB2-GST[b]	$cdc42^{Y40C,Q61L}$	This study
pDLB1322	pHB2-GST[b]	$cdc42^{Y40K,Q61L}$	This study
pDLB1323	*CEN URA3*	$cdc42^{D38I}$	This study
pDLB1656	2 μm *URA3*	$cdc42^{T35A}$	This study
pDLB1657	2 μm *URA3*	$cdc42^{V36A}$	This study
pDLB1658	2 μm *URA3*	$cdc42^{V36T}$	This study
pDLB1659	2 μm *URA3*	$cdc42^{F37G}$	This study
pDLB1660	2 μm *URA3*	$cdc42^{F37Y}$	This study
pDLB1661	2 μm *URA3*	$cdc42^{D38A}$	This study
pDLB1662	2 μm *URA3*	$cdc42^{D38I}$	This study
pDLB1663	2 μm *URA3*	$cdc42^{N39A}$	This study
pDLB1664	2 μm *URA3*	$cdc42^{Y40C}$	This study
pDLB1665	2 μm *URA3*	$cdc42^{Y40K}$	This study
pDLB1666	2 μm *URA3*	*CDC42*	This study
pDLB1723	2 μm *TRP1*	$cdc42^{T35A}$	This study
pDLB1724	2 μm *TRP1*	$cdc42^{V36A}$	This study
pDLB1726	2 μm *TRP1*	$cdc42^{F37G}$	This study
pDLB1727	2 μm *TRP1*	$cdc42^{F37Y}$	This study
pDLB1728	2 μm *TRP1*	$cdc42^{D38A}$	This study
pDLB1729	2 μm *TRP1*	$cdc42^{D38I}$	This study
pDLB1730	2 μm *TRP1*	$cdc42^{N39A}$	This study
pDLB1731	2 μm *TRP1*	$cdc42^{Y40C}$	This study
pDLB1732	2 μm *TRP1*	$cdc42^{Y40K}$	This study
pDLB1733	2 μm *TRP1*	*CDC42*	This study
pDLB1861	pHB1-myc3[b]	*CLA4* CRIB	This study
pMOSB14	pCR2.1[c]	$cdc42^{V36T}$	This study
pMOSB15	pCR2.1[c]	$cdc42^{T35A}$	This study
pMOSB16	pCR2.1[c]	$cdc42^{V36A}$	This study
pMOSB17	pCR2.1[c]	$cdc42^{D38A}$	This study
pMOSB18	pCR2.1[c]	$cdc42^{F37Y}$	This study
pMOSB19	pCR2.1[c]	$cdc42^{F37G}$	This study
pMOSB23	pCR2.1[c]	$cdc42^{Y40K}$	This study
pMOSB26	pCR2.1[c]	$cdc42^{D38I}$	This study
pMOSB27	pCR2.1[c]	$cdc42^{N39A}$	This study
pMOSB53	pCR2.1[c]	$cdc42^{Y40C}$	This study
pMOSB40	*CEN URA3*	$cdc42^{F37G}$	This study
pMOSB41	*CEN URA3*	$cdc42^{Y40K}$	This study
pMOSB45	*CEN TRP1*	*CDC42*	This study
pMOSB46	*CEN TRP1*	$cdc42^{T35A}$	This study
pMOSB47	*CEN TRP1*	$cdc42^{V36A}$	This study
pMOSB48	*CEN TRP1*	$cdc42^{F37G}$	This study
pMOSB49	*CEN TRP1*	$cdc42^{D38I}$	This study
pMOSB50	*CEN TRP1*	$cdc42^{D38A}$	This study
pMOSB51	*CEN TRP1*	$cdc42^{Y40K}$	This study
pMOSB55	*CEN URA3*	*CDC42*	This study
pMOSB57	*CEN URA3*	$cdc42^{V36T}$	This study
pMOSB58	*CEN URA3*	$cdc42^{F37Y}$	This study
pMOSB59	*CEN URA3*	$cdc42^{N39A}$	This study
pMOSB175	*CEN TRP1*	$cdc42^{Y40C}$	This study
pMOSB176	*CEN URA3*	$cdc42^{Y40C}$	This study
pMOSB177	*CEN URA3*	$cdc42^{V36A}$	This study
pMOSB186	*CEN URA3*	$cdc42^{T35A}$	This study
pMOSB229	2 μm *URA3*	*GIC1*	Matthias Peter
pMOSB230	2 μm *URA3*	*GIC2*	Jaquenoud *et al.* (1998)
pMOSB240	pGEX	*STE20* CRIB	Moskow *et al.* (2000)
pRS314	*CEN TRP1*		Sikorski and Hieter (1989)
pRS316	*CEN URA3*		Sikorski and Hieter (1989)
pRS426	2 μm *URA3*		Christianson *et al.* (1992)
pRS424	2 μm *TRP1*		Christianson *et al.* (1992)
YEp24	2 μm *URA3*		New England Biolabs (Beverly, MA)

[a] Isolated from Yep24 genomic library. Insert containing full-length *CDC24* was confirmed by sequencing.

[b] Univector and host plasmids as previously described (Liu *et al.*, 1998).

[c] pCR2.1 from Invitrogen (San Diego, CA).

Table 3. Oligonucleotides used in this study

Oligo	Description	Oligonucleotide sequence
cdc-1[a]	*cdc42-T35A*	**G**CAGTGTTCGATAACTATGC
cdc-3[a]	*cdc42-V36T*	ACA**AC**GTTCGATAACTATGCGG
cdc-4[a]	*cdc42-V36A*	ACA**GC**GTTCGATAACTATGCGG
cdc-5[a]	*cdc42-F37Y*	ACAGTGT**A**CGATAACTATGCGGTG
cdc-6[a]	*cdc42-F37G*	ACAGTG**GG**CGATAACTATGCGGTG
cdc-7[a]	*cdc42-D38I*	ACAGTGTTC**AT**TAACTATGCGGTGACTG
cdc-8[a]	*cdc42-D38A*	ACAGTGTTCG**C**TAACTATGCGGTGACTG
cdc-9[a]	*cdc42-N39A*	ACAGTGTTCGAT**GC**CTATGCGGTGACTGTG
cdc-10[a]	*cdc42-Y40K*	ACAGTGTTCGATAAC**A**A**G**GCGGTGACTGTGATG
cdc-11[b]	reverse primer	TGGAACATAGTCAGCTGGAAATTGATTCG
cdc-22[a]	*cdc42-Y40C*	ACAGTGTTCGATAACT**G**TGCGGTGACTGTGATG
DJL42-3	*CDC42* promoter	CCACCGTCGATTCAAGGGTC
DJL42-6	*TDH3* terminator	CTACTACAGATATTACATGTGGCG
DJL42-4	*CDC42* stop	GCGAAACGAGTCTCTAGA
CLA4-UNI1[c]	*CLA4*-CRIB/*Nde*I	GGAATTCCATATGGATTTGCATAGTTGGTTAGACGCC
CLA4-UNI2[c]	*CLA4*-CRIB/*Sac*I	CCGACTCTCAATCTTCTCCTGTAATTCTGGAGTG
GIC1-UNI1[c]	*GIC1*-CRIB/*Nde*I	GGAATTCCATATGCTGTTGTCGAGGAGACATGGGTCTGCC
GIC1-UNI2[c]	*GIC1*-CRIB/*Sac*I	CCGAGCTCTCATGGTCGGGGTTGCGGTGCCAAAGACG
GIC2-UNI1[c]	*GIC2*-CRIB/*Nde*I	GGAATTCCATATGGGTGCCCAACCGGACATAAGAGGT
GIC2-UNI2[c]	*GIC2*-CRIB/*Sac*I	CCGAGCTCTCAGGTATAGTCGTCCTTAATCTCTGTGG
BEM1-2	*BEM1*	GATCCATATGCTGAAAAACTTCAAACTC
BEM1-3	*BEM1*	GCTTCGTCTTCTAACACTAG

[a] Sequence changes are indicated by bases in boldface.

[b] cdc-11 has a silent mutation that introduces a *Pvu*II site (underlined).

[c] Underlined sequences indicate *Nde*I and *Sac*I restriction sites used for cloning.

Two strategies were taken to integrate the *cdc42* alleles into the genome. First, a linear 1-kb *Eco*RI fragment containing the promoter and open reading frame of the mutant was transformed together with an uncut pRS314 "carrier" plasmid into strain MOSY0090, which contains a *cdc42::URA3* disruption (missing all but the last 78 bp of the *CDC42* open reading frame) at the *CDC42* locus and a copy of *CDC42* under control of the *GAL1* promoter at the *LEU2* locus (Moskow *et al.*, 2000). Trp+ transformants containing the carrier plasmid were first selected on galactose-containing plates lacking tryptophan, and then those transformants in which the *cdc42* allele had replaced the *cdc42::URA3* deletion were selected by replica-plating onto dextrose-containing plates with 5-fluoroorotic acid, which kills *URA3* cells. Gene replacement was confirmed by PCR with the oligonucleotides DJL42-3 and DJL42-4, which amplify a 1-kb product from the effector-loop alleles but not from *cdc42::URA3* (lacking the region complementary to DJL42-4) or *GAL1p-CDC42* (lacking the promoter region complementary to DJL42-3). Haploid mutants were backcrossed to a wild-type strain, and the *cdc42* phenotypes (see text) were observed to segregate 2:2 in at least 10 tetrads, indicating that the phenotypes are caused by the *cdc42* allele alone (and not due to second site mutations).

This strategy was successful for the *cdc42*^{V36A}, *cdc42*^{V36T}, and *cdc42*^{N39A} alleles, but we were unable to apply the 5-fluoroorotic selection on galactose-containing plates (Ura+ cells grew on such plates), so the above-described strategy was not workable for *cdc42* alleles that were unable to support growth on dextrose (i.e., as the sole copy of *CDC42*). In an alternative strategy, the 1-kb *Eco*RI fragments containing the effector-loop alleles were cloned into the *Eco*RI site of the integrating vector YIpGAP2 (Sia *et al.*, 1996), which contains the *HIS2* marker in a pUC18 backbone. The resulting plasmids were digested with *Xba*I, which cuts at a unique site within *HIS2*, and transformed into strain DLY3067 (Moskow *et al.*, 2000), in which the genomic *CDC42* is placed under control of the *GAL1* promoter. Integration of the mutant alleles at *HIS2* in His+ transformants (selected on galactose-containing plates) was confirmed by PCR as described above. The same strategy was used to introduce the alleles into strain MOSY0121 (*cdc42-6*). The phenotype of each mutant was identical whether it was analyzed by glucose shift (depleting wild-type Cdc42p in the *GAL1p-CDC42* strains) or by temperature shift (inactivating Cdc42-6p in *cdc42-6* strains).

The *cdc42-6* allele was generated by the same PCR mutagenesis and gap repair strategy described for isolation of pheromone-resistant *cdc42-md* alleles (Moskow *et al.*, 2000) except that transformants were screened for temperature-sensitive growth rather than pheromone resistance. *cdc42-6* was then integrated at the genomic *CDC42* locus by the *cdc42::URA3* replacement strategy described above. The resulting *cdc42-6* strain grows well at 23°C but arrests with a uniform large round unbudded cell phenotype at 37°C. The minimal restrictive temperature for this strain is 33°C, but we shifted the cells to 37°C to eliminate as much residual function as possible. We first characterized the tightness of this mutant by staining cells grown at the permissive temperature with fluorescein isothiocyanate-concanvalin A (a vital stain for cell wall polysaccharide (Adams and Pringle, 1984) and then shifting them to 37°C in medium lacking fluorescein isothiocyanate-concanvalin A. Any buds formed after the temperature shift would then appear as dark buds attached to bright green mother cells, allowing an accurate estimate of how rapidly bud formation ceased after temperature shift. By this criterion, <5.0% of *cdc42-6* cells initiated bud formation after the shift to 37°C (in comparison >20% of *cdc42-1* cells did so), indicating a tight and fast-acting phenotype for this mutant.

To express GTP-locked versions of the effector-loop Cdc42p variants in bacteria, double mutant alleles containing an additional Q61L substitution were generated by a "gap-repair" strategy and then cloned into the "univector" pUNI-10 (Liu *et al.*, 1998) as described previously for pheromone-resistant *cdc42* alleles (Moskow *et al.*, 2000). These plasmids were then recombined with the "host" vector pHB1-MYC3 (Liu *et al.*, 1998) by using Cre recombinase in vitro, generating bacterial expression plasmids directing production of double-mutant alleles fused to three c-myc epitopes at the N

Table 4. Crosses used for complementation analysis[a]

	T35A	V36T	V36A	F37G	F37Y	D38A	D38I	N39A	Y40C	Y40K
T35A	3511 × 3809	3500 × 3809	3497 × 3809	3517 × 3809	3881 × 3809	3515 × 3809	3509 × 3809	3496 × 3809	3519 × 3809	3513 × 3809
V36A	3511 × 3554	3500 × 3554	3497 × 3554	3517 × 3554	3881 × 3554	3515 × 3554	3509 × 3554	3496 × 3554	3519 × 3554	3513 × 3554
V36T	3511 × 3553	3500 × 3553	3497 × 3553	3517 × 3553	3881 × 3553	3515 × 3553	3509 × 3553	3496 × 3553	3519 × 3553	3513 × 3553
F37G	3809 × 3517	3553 × 3517	3554 × 3517	3517 × 3579	3880 × 3517	3515 × 3579	3509 × 3579	3556 × 3517	3540 × 3517	3513 × 3579
F37Y	3511 × 3880	3500 × 3880	3497 × 3880	3517 × 3880	3881 × 3880	3515 × 3880	3509 × 3880	3496 × 3880	3519 × 3880	3513 × 3880
D38A	3515 × 3809	3553 × 3515	3554 × 3515	3517 × 3541	3880 × 3515	3515 × 3541	3509 × 3541	3556 × 3515	3540 × 3515	3513 × 3541
D38I	3509 × 3809	3553 × 3509	3554 × 3509	3517 × 3804	3880 × 3509	3515 × 3804	3509 × 3804	3556 × 3509	3540 × 3509	3513 × 3804
N39A	3511 × 3556	3500 × 3556	3497 × 3556	3517 × 3556	3881 × 3556	3515 × 3556	3509 × 3556	3496 × 3556	3519 × 3556	3513 × 3556
Y40C	3511 × 3525	3500 × 3525	3497 × 3525	3517 × 3525	3881 × 3525	3515 × 3525	3509 × 3525	3496 × 3525	3519 × 3525	3513 × 3525
Y40K	3513 × 3809	3553 × 3513	3554 × 3513	3517 × 3540	3880 × 3513	3515 × 3540	3509 × 3540	3556 × 3513	3525 × 3513	3513 × 3540

[a] All numbers are DLY strains listed in Table 1.

terminus. To express the effector CRIB domains, the relevant regions of *CLA4* (amino acids 164–225), *GIC1* (amino acids 109–171), and *GIC2* (amino acids 124–172) were amplified by PCR with yeast genomic DNA as template and the oligonucleotides listed in Table 3. PCR products were digested with *Nde*I and *Sac*I and cloned into the corresponding sites of pUNI-10. To express full-length Bem1p, the entire *BEM1* gene was amplified from yeast genomic DNA by using the BEM1-2 and BEM1-3 oligonucleotides listed in Table 3. The resulting PCR fragment was cloned into pCR2.1 (Invitrogen), and a *Nde*I/*Xho*I *BEM1* fragment was then cloned into the *Nde*I/*Sal*I sites of pUNI-10. All pUNI constructs were sequenced to confirm that no additional mutations occurred as a result of PCR manipulations. pUNI*GIC1* CRIB, pUNI*GIC2* CRIB, and pUNI*BEM1* were then recombined with the host vector pHB2-GST (Liu *et al.*, 1998), generating a bacterial expression plasmid directing production of Bem1p fused to GST at the N terminus. pUNI*CLA4* CRIB was recombined with pHB1-MYC3 (Liu *et al.*, 1998) to express a fusion protein. The plasmid pGEX-Ste20CRIB (Moskow *et al.*, 2000) was used to express the region encoding Ste20p amino acids 328–428 fused to glutathione *S*-transferase (GST) at the N terminus.

Media, Growth Conditions, and Depletion of Wild-Type Cdc42p

Strains were grown in YEPD (1% yeast extract, 2% bacto-peptone, 2% dextrose, and 0.01% adenine), YEPG (as YEPD but with 2% galactose instead of dextrose), or (for strains containing plasmids) drop-out medium (Guthrie and Fink, 1991) lacking uracil, tryptophan, or histidine, as appropriate. For strains containing both an effector-loop allele of *CDC42* under control of the *CDC42* promoter and a wild-type copy of *CDC42* under control of the *GAL1* promoter, the wild-type Cdc42p was depleted by growth of the cells in dextrose-containing medium for at least 24 h. Control experiments confirmed that this was sufficient to deplete the protein to undetectable levels and to produce a uniform unbudded arrest in cells lacking an additional copy of *CDC42*.

Intragenic Complementation Analysis

The crosses performed to generate the intragenic complementation strains are listed in Table 4. Starting haploid strains contained the relevant effector-loop allele of *CDC42* and an additional copy of either *GAL1p-CDC42* or the temperature-sensitive *cdc42-6* allele. Intragenic complementation was evaluated on dextrose medium (to deplete *GAL1p-CDC42* where relevant) at 37°C (to inactivate *cdc42-6*). For the *GAL1p-CDC42* strains the analysis was also performed at 37°C, with identical results. To evaluate intragenic complementation at higher copy-number, DLY3067 was transformed with pairwise combinations of alleles on *TRP1* and *URA3* marked plasmids. Wild-type Cdc42p was depleted by growth for 30 h at 30°C on dextrose medium before evaluating complementation.

Quantitation of Cdc42p Expression in Yeast

Centromeric plasmids directing expression of *CDC42* alleles were transformed into the *cdc42-1* strain DLY680. Cdc42-1p is expressed at very low levels (Ziman *et al.*, 1991; Kozminski *et al.*, 2000), so that detectable signals by Western blot represent the abundance of Cdc42p expressed from the plasmid. Strains were grown in YEPD at 24°C, so that Cdc42-1p was able to provide the functions necessary for viability and the blot reflects the abundance of Cdc42p effector-loop variants in proliferating cells. Yeast cells were then harvested by centrifugation and protein extracts were prepared by resuspending the pellets in NP-40 lysis buffer (50 mM Tris-HCl [pH 7.5], 150 mM NaCl, 5 mM EDTA, 1% NP-40, 1 mM sodium pyrophosphate, 1 mM phenylmethylsulfonyl fluoride, 1 mM sodium orthovanadate, and 2 μg/ml each of pepstatin A and leupeptin [Sigma, St. Louis, MO]) and vortexing with acid-washed glass beads. Lysates were clarified by centrifugation for 10 min at 14,000 rpm in an Eppendorf microfuge at 4°C. Protein concentration was determined by the Bradford method (Bio-Rad, Hercules, CA), and equal amounts of total protein were resolved by SDS-PAGE and immunoblotted using polyclonal rabbit anti-Cdc42p antibody (diluted 1/500) kindly provided by Patrick Brennwald, and horseradish peroxidase-conjugated goat anti-rabbit secondary antibody (diluted 1/2000). As a loading control, filters were subsequently incubated with monoclonal anti-PSTAIRE antibody (Yamashita *et al.*, 1991) (ascites preparation diluted 1/20000), which recognizes both Cdc28p and Pho85p in yeast, and horseradish peroxidase-conjugated goat anti-mouse secondary antibody (diluted 1/2000). Blots were developed using the Renaissance Chemiluminescence Reagent Plus (PerkinElmer Life Science Products, Boston, MA).

Immunofluorescence and Other Microscopic Analysis

Overall cell morphologies were examined by differential-interference-contrast microscopy, and cells were stained with 4,6-diamidino-2-phenylindole (Sigma) to visualize DNA (Pringle, 1991), with 10 μg/ml Calcofluor (Sigma) to visualize chitin (Pringle, 1991), or with rhodamine-phalloidin (Molecular Probes, Eugene, OR) to visualize F-actin (Bi *et al.*, 1998). To visualize septins, cells were fixed by addition of formaldehyde (3.7% final concentration) to the medium and incubated for 75 min at 30°C before processing for immunofluorescence as described previously (Pringle, 1991). Rabbit anti-Cdc11p antibody (Santa Cruz Biotechnology, Santa Cruz, CA) was used at 1/10 dilution and Cy2-conjugated goat anti-rabbit secondary antibody was used at a 1/100 dilution (Jackson Immu-

noresearch Laboratories, West Grove, PA). To localize Cdc42p, cells were fixed for 2.5 h in as described (Lehman *et al.*, 1999). Fixed cells were incubated with 0.5% SDS and processed for immunofluorescence as described (Redding *et al.*, 1991). Anti-Cdc42p antibody (used at 1/100 dilution) was generously provided by Patrick Brennwald. Cells were examined using a Zeiss Axioscop. Images were captured using a Pentamax cooled charge-coupled device camera (Princeton Instruments, Princeton, NJ), interfaced with MetaMorph software (Universal Imaging, Silver Spring, MD).

Production of Recombinant Proteins and Binding Assays

Plasmids directing expression of myc-tagged *cdc42* alleles were transformed into *Escherichia coli* BL21(DE3) (Stratagene) and GST-tagged effectors were transformed into *E. coli* BL21. Extracts were prepared as described previously (Moskow *et al.*, 2000). To ensure that binding reactions contained equal amounts of each effector-loop variant, titration series of each bacterial extract containing Cdc42p-myc were resolved by SDS-PAGE, transferred to Immobilon-P nylon membrane (Millipore, Bedford, MA), and immunoblotted with monoclonal anti-myc antibodies (9E10; Santa Cruz Biotechnology) by using standard procedures (Ausubel *et al.*, 1995). Lysate concentrations were then adjusted so that equal amounts of each Cdc42p-myc variant were added to the binding reactions. GST-effectors were purified using glutathione Sepharose 4B (Amersham Pharmacia Biotech, Piscataway, NJ), and the beads were incubated together with the normalized bacterial extracts containing Cdc42p-myc, washed, and analyzed to detect bound Cdc42p as described previously (Moskow *et al.*, 2000), except that 125 mM NaCl was added to the wash buffer. A modification of this strategy was used for Cla4p because the GST-tagged Cla4p CRIB domain did not display specific binding to myc-tagged Cdc42p. In this case the procedure was reversed and GST-tagged Cdc42p variants were immobilized on beads and incubated with bacterial lysates expressing myc-tagged Cla4p CRIB domain. GST-tagged protein concentrations were normalized using the Bradford assay (Bio-Rad). In all cases, india ink staining of the blots confirmed that equal amounts of GST-tagged proteins were present in each set of binding assays.

RESULTS

Generation of Effector-Loop Mutants of CDC42

The effector loop comprises the "Switch I" region (residues 30–40) of Cdc42p, one of two regions that assume different conformations depending on whether the protein is GDP- or GTP-bound (Wittinghofer and Nassar, 1996). The most commonly used "effector" mutation, altering Thr35 to Ala, is thought to block binding of all effectors to small G proteins and affects coordination of the Mg^{2+} ion in the complex (Pai *et al.*, 1990). Other mutations in this region of Ras were shown to partially attenuate the transforming potential of oncogenic Ras by crippling specific downstream pathways (Joneson and Bar-Sagi, 1997). Subsequent studies on Rho, Rac, and Cdc42p confirmed that similar selective effects could be obtained by mutating this region in members of the Rho subfamily (Diekmann *et al.*, 1995; Nobes and Hall, 1995; Lamarche *et al.*, 1996). Based on the available literature we generated the T35A mutant and nine more mutants (Figure 1) by site-directed mutagenesis. Initially, we introduced a single copy of each mutant under control of the *CDC42* promoter into the genome of a strain containing a second copy of (wild-type) *CDC42* under control of the regulatable *GAL1* promoter (see MATERIALS AND METHODS for details). Growth of this strain in dextrose-containing medium promotes repression of the *GAL1* promoter, permitting analysis of the phenotypes of strains expressing only the mutant forms of Cdc42p. Control experiments showed that wild-type Cdc42p was depleted within 10 generations of a shift from galactose-to dextrose-containing medium, and cells lacking a second copy of *CDC42* arrested uniformly as large, round, unbudded cells with depolarized actin and no assembled septin structures (similar to the *cdc42-1* arrest phenotype at the restrictive temperature [Adams *et al.*, 1990]). Of the 10 effector-loop alleles, four were able to sustain cell proliferation when present as the only expressed copy of *CDC42*, whereas six others were not (Figure 1A). The inviability of these six mutants was recessive to wild type (our unpublished results), consistent with impairment of the function of at least one essential effector pathway. In addition, the inviability of the mutants was not suppressed by incubation at low temperature (14°C) or in media of elevated osmolarity (supplemented with 1 M sorbitol or 1 M NaCl) (our unpublished results). None of the other four mutants were temperature-sensitive (37°C) or cold-sensitive (14°C) for viability and only $cdc42^{V36T}$ grew somewhat slower than wild type at 37°C. The phenotypes of these mutants were not significantly enhanced or suppressed on media with elevated osmolarity (our unpublished results).

To determine the level of expression of the Cdc42p variants encoded by the effector-loop alleles, we expressed each variant in a *cdc42-1* strain. It has been shown that despite its ability to sustain cell proliferation at 24°C, Cdc42-1p is expressed at very low levels (Ziman *et al.*, 1991; Kozminski *et al.*, 2000), providing a very low background signal (Figure 1B). Most of the effector-loop variants were expressed at approximately similar levels to the wild type (Figure 1B), indicating that phenotypic differences are unlikely to stem simply from differences in expression level.

Wild-type Cdc42p is concentrated at the bud site and at the bud tips of cells with small buds (Ziman *et al.*, 1993). To determine whether the Cdc42p variants encoded by the effector-loop alleles were able to localize to these sites we again expressed the variants in a *cdc42-1* strain, providing a very low background in which localization of other Cdc42p variants could be detected (Figure 1C). Perhaps surprisingly, all of the Cdc42p variants could be found localized at the bud site and at the bud tips at 24°C (Figure 1C). This suggests that effector interactions are not critical for Cdc42p localization. However, polarity functions provided by Cdc42-1p may contribute to localization of the other Cdc42p variants in these strains. In addition, we only detected Cdc42p staining in a minority of cells even for wild-type Cdc42p, and it appeared that signals from the variants might be qualitatively less frequent and/or intense.

Phenotypic Characterization of Effector-Loop Mutants

Polarization of yeast cells before budding is triggered by activation of the cyclin-dependent kinase Cdc28p by G1 cyclins (Lew and Reed, 1993). Upon Cdc28p activation, Cdc42p becomes concentrated beneath a patch of plasma membrane at the presumptive bud site (Ziman *et al.*, 1993). At about the same time, the actin cables become oriented, cortical actin patches are clustered, septins (filament-forming proteins that remain at the mother-bud neck during subsequent bud growth) assemble into a ring, and several other proteins including the "polarisome" components

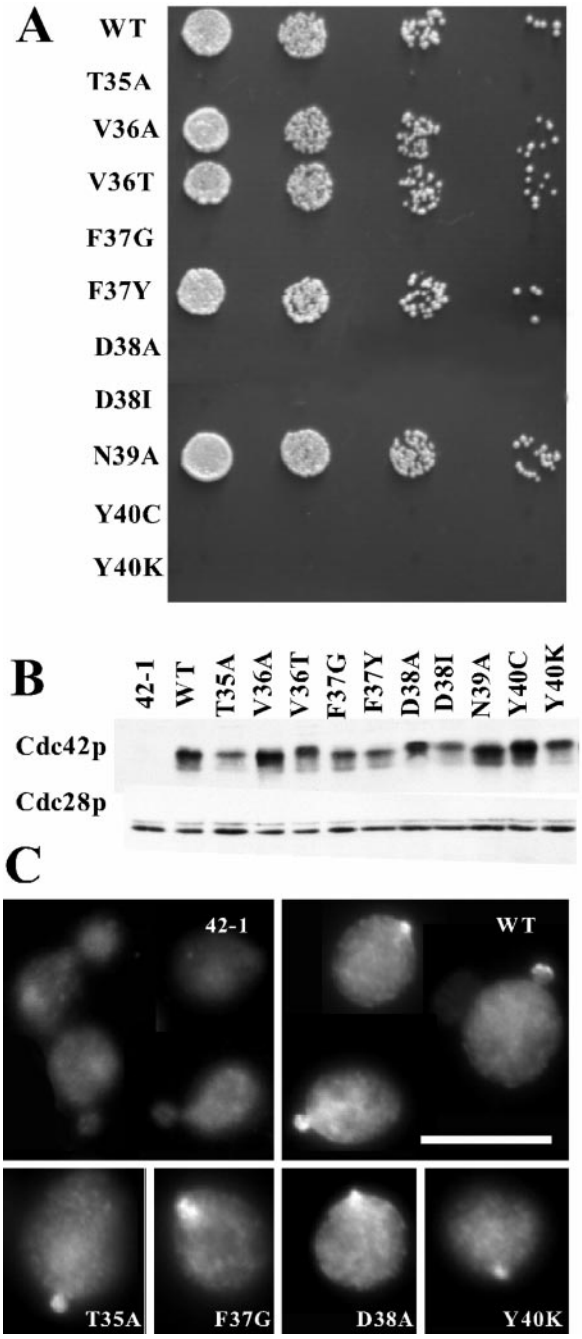

Figure 1. Characterization of *cdc42* effector-loop alleles. (A) Wild-type (DLY1) and *cdc42* effector-loop mutant strains DLY3511 (T35A), DLY3497 (V36A), DLY3500 (V36T), DLY3517(F37G), DLY3881 (F37Y), DLY3515 (D38A), DLY3509 (D38I), DLY3496(N39A), DLY3519 (Y40C), and DLY3513 (Y40K) were grown in YEPD at 30°C for 24 h to deplete wild-type Cdc42p expressed from the *GAL1* promoter. Cells were counted with a hemacytometer and fivefold serial dilutions were spotted onto a YEPD plate, which was incubated for 36 h at 30°C. (B) Strain DLY680 (*cdc42-1*) was transformed with plasmids expressing the indicated *cdc42* alleles pMOSB55 (WT), pMOSB186 (T35A), MOSB177(V36A), pMOSB57(V36T), pMOSB40 (F37G), pMOSB58 (F37Y), pMOSB50(D38A), pDLB1323 (D38I), pMOSB59(N39A), pMOSB176 (Y40C), and pMOSB41 (Y40K). Cells were grown to exponential phase in YEPD at 24°C. Lysates were prepared and analyzed by immunoblotting with anti-Cdc42p or anti-PSTAIRE antibodies (to control for loading). (C) The same strains used in B were grown to exponential phase in YEPD at 24°C and processed to visualize localization of Cdc42p. Bar, 10 μm.

Bni1p and Spa2p congregate in a patch at the prebud site (Pringle *et al.*, 1995; Johnson, 1999). All of these polarized distributions require Cdc42p activity; conversely, Cdc42p polarization does not require F-actin, assembled septins, or polarisome components. In addition, the F-actin, septin, and polarisome reorganizations are mutually independent: elimination of one does not affect polarization of the others (Pringle *et al.*, 1995; Ayscough *et al.*, 1997). These findings suggest that Cdc42p promotes the independent polarization of several cytoskeletal structures, perhaps through separate effector pathways. At least two of these polarization targets (F-actin and septins) are essential for yeast viability. We examined the phenotypes of the effector-loop *cdc42* mutants with respect to cell morphology, F-actin organization, and septin organization after depletion of the wild-type Cdc42p on dextrose medium (Figure 2). These are described below, going from least to most severe.

Cells containing the *cdc42*^{F37Y} or *cdc42*^{N39A} alleles were generally wild type with respect to cell morphology, actin organization, and septin organization. At low penetrance (<10% of cells), *cdc42*^{N39A} cells displayed lumps protruding from the base of the bud or aberrant septin staining, but these defects were subtle. Previous studies indicated that perturbation of actin organization could cause defects in the bipolar pattern of bud site selection observed in diploid cells (Yang *et al.*, 1997), whereas perturbation of septin organization could cause defects in the axial pattern of bud site selection observed in haploid cells (Flescher *et al.*, 1993). We found that *cdc42*^{F37Y} and *cdc42*^{N39A} mutant cells displayed normal bipolar bud site selection in diploids but were mildly defective in axial bud site selection in haploids (Figure 2B). Thus, any effector pathways compromised in these mutants are not critical for cytoskeletal organization.

Cells containing the *cdc42*^{V36T} or *cdc42*^{V36A} alleles displayed apparently normal actin organization but had wide and misshapen mother-bud necks and poorly organized septins (Figure 2A). These defects were qualitatively similar for both mutants but were more penetrant and more severe in *cdc42*^{V36T} cells. The most frequent defect was a wider neck (67% of *cdc42*^{V36T} cells, n = 200), and at lower frequencies knobby, kinked, or stretched necks were observed (often in the same cells that had wider necks). In cells with wide necks, septin staining was generally fainter, patchy, and occasionally even undetectable at the neck, and in some cases septin staining was observed at the tip of the bud (36% of cells, n = 200). Aberrant septin staining was observed for three different septins: Cdc11p (Figure 2A), Cdc3p (detected using anti-Cdc3p antibody or Cdc3p-GFP; data not shown), and Cdc12p (detected using Cdc12p-GFP; data not shown). In addition, calcofluor staining revealed a severe defect in the localization of chitin deposition, which is guided by the underlying septin ring, in *cdc42*^{V36T} mutants (Figure 2C). These defects included increased staining all over the cell wall, broader and irregular zones of bright staining at the neck, and bright uneven staining in the vicinity of bud scars.

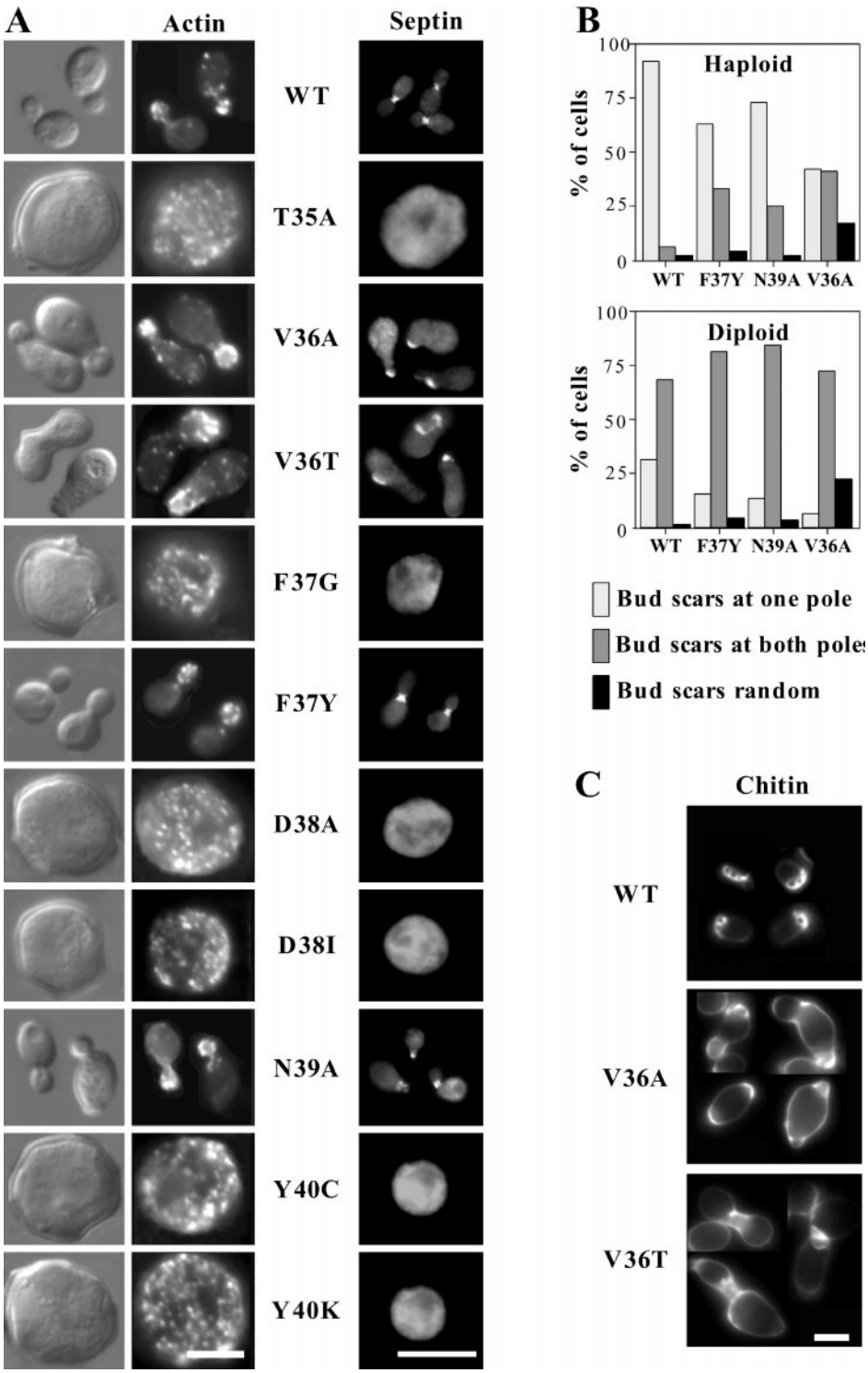

Figure 2. Phenotype of *cdc42* effector-loop alleles. (A) Cell morphology, F-actin and septin distribution in *cdc42* effector-loop mutants. DLY1 (WT), DLY3511 (T35A), DLY3497 (V36A), DLY3500 (V36T), DLY3517 (F37G), DLY3881 (F37Y), DLY3515 (D38A), DLY3509 (D38I), DLY3496 (N39A), DLY3519 (Y40C), and DLY3513 (Y40K) strains were grown in YEPD at 30°C for 36 h, fixed, and stained with rhodamine-phalloidin (actin) or anti-Cdc11p (septin) as described in MATERIALS AND METHODS. Bar, 5 μm. (B) Bud-site selection in *cdc42* effector-loop mutants. Haploid DLY1 (WT), DLY3881 (F37Y), DLY3496 (N39A), and DLY3497 (V36A) strains and diploid DLY5 (WT), DLY4756 (F37Y), DLY4757 (N39A), and DLY3923 (V36A) strains were grown to exponential phase in YEPD at 30°C, and stained with calcofluor to visualize bud scars. Cells with two or more bud scars were scored as having scars at only one pole (expected for axial or bipolar budding), at both poles (expected

Similar but less severe defects were observed in *cdc42*^{V36A} mutants (Figure 2C), which also displayed a severe axial bud site selection defect (Figure 2B). All of the septin defects were corrected in *cdc42*^{V36A}/*CDC42* and *cdc42*^{V36T}/*CDC42* heterozygotes (our unpublished results), indicating that these are loss-of-function alleles that are defective in pathways important for neck morphology and septin organization.

For each of the six effector-loop alleles that could not sustain cell proliferation, the populations arrested uniformly as large, round, unbudded cells with depolarized actin patches and no detectable assembled septins, similar to the arrest observed in the absence of Cdc42p (Figure 2A). This is thought to be the *cdc42* null phenotype, and suggests that each of these alleles has crippled interactions with crucial effectors of Cdc42p.

Effect of Increased Gene Dosage on Phenotype of Effector-Loop Mutants

The findings described above seemed rather surprising, in that several mutant alleles that had been described as specific partial function mutants in other G proteins (including in some cases similar alleles of human *CDC42* [Lamarche *et al.*, 1996]) appeared to behave as null alleles (Figure 2). However, a significant difference with prior studies was that in this study the alleles were expressed at single copy from the endogenous promoter. In contrast, most previous reports either overexpressed or injected large amounts of proteins encoded by alleles that also contained a second mutation locking the protein in the GTP-bound form. These considerations suggested at least two possible reasons for the apparent discrepancies. First, it seemed possible that the more severe alleles had (in addition to some specific defects in effector interaction) a general defect in GTP-loading, which would render them inactive in our study but not when GTP hydrolysis was inhibited. Second, it seemed possible that the proteins encoded by these alleles might have global, general defects in effector interactions superimposed upon a more specific defect. In either case, assaying mutant phenotypes when the alleles are expressed at single copy would reveal the general defect, whereas overexpression might overcome the global defect but now reveal more specific phenotypic defects. To address this possibility, we subcloned the effector-loop alleles (still expressed from the *CDC42* promoter) into low- and high-copy vectors (CEN ARS and 2 μm, respectively).

We found that *cdc42*^{Y40C} and *cdc42*^{F37G} were able to sustain some proliferation (albeit poorly) when expressed from a low-copy plasmid, and that proliferation was significantly improved when the alleles were expressed from a high-copy plasmid (Figure 3A). In addition, *cdc42*^{Y40K} was able to sustain proliferation when expressed from a high-copy plasmid, though not from a low-copy plasmid (Figure 3A). However, *cdc42*^{T35A}, *cdc42*^{D38I}, and *cdc42*^{D38A} were unable to sustain proliferation even when expressed from high-copy plasmids (Figure 3A; data not shown).

Even when overexpressed, *cdc42*^{Y40C}, *cdc42*^{Y40K}, and *cdc42*^{F37G} mutants displayed severe defects in cell morphology. In all three cases, the mutants were generally larger and rounder than wild-type cells (Figure 3, B and C). About half of the cells containing the high-copy *cdc42*^{Y40C} plasmid exhibited depolarized actin patches and slightly fainter actin cables, although when visible most actin cables were polarized (Figure 3B). Additionally, knots of actin "ropes" that appeared brighter and thicker than normal actin cables were observed in about half of the budded cells (though these were not correlated with depolarized patches; Figure 3B). Cells containing the high-copy *cdc42*^{Y40K} displayed a more severe depolarization of actin patches (73% of cells, n = 200), but ropes were not detected (Figure 3B). Both the high-copy *cdc42*^{Y40C} (40% of unbudded cells, n = 131) and the high-copy *cdc42*^{Y40K} (29% of unbudded cells, n = 148) cell populations contained binucleate or multinucleate cells as judged by 4,6-diamidino-2-phenylindole staining. Septin organization in cells containing high-copy *cdc42*^{Y40C} or high-copy *cdc42*^{Y40K} plasmids was relatively normal: the septin rings were always localized to the neck, but they sometimes appeared broader than in wild-type cells (Figure 3C). Cells expressing high-copy *cdc42*^{F37G} generally contained polarized actin patches (80% of cells, n = 200) and cables, though the cables appeared fainter than in wild-type cells (Figure 3B). These cells also had fewer multinucleate cells (15% of unbudded cells, n = 125). Septin rings were localized to the neck, but were frequently faint (49% of the cells, n = 200) and the septin ring often had diffuse tendrils of septin staining extending out from the ring perpendicular to the neck (30% of the cells, n = 200; Figure 3C). Such tendrils were not observed in the *cdc42*^{Y40C} and *cdc42*^{Y40K} strains. Thus, at high gene dosage *cdc42*^{Y40C} and *cdc42*^{Y40K} show relatively specific defects in actin organization, whereas *cdc42*^{F37G} shows more subtle defects in both actin and septin organization.

Intragenic Complementation among Effector-Loop Alleles

We generated heterozygous diploid strains containing all possible pairs of *cdc42* effector-loop alleles (see MATERIALS AND METHODS) to ask whether they had defects in separate or overlapping functions of Cdc42p. Heterozygotes containing the pseudo wild-type alleles *cdc42*^{F37Y} and *cdc42*^{N39A} together with any other allele appeared wild type, as expected (our unpublished results). Heterozygotes containing the two alleles displaying neck organization defects (*cdc42*^{V36A} and *cdc42*^{V36T}) were phenotypically similar to homozygotes for the milder allele (*cdc42*^{V36A}), indicating that these alleles affect similar pathways (our unpublished results).

All of the heterozygotes between severe effector-loop alleles (*cdc42*^{T35A}, *cdc42*^{F37G}, *cdc42*^{D38I}, *cdc42*^{D38A}, *cdc42*^{Y40C}, or *cdc42*^{Y40K}) arrested with a similar phenotype to the starting haploids (large, round, unbudded cells lacking polarized actin or assembled septins; our unpublished results). This result suggests that all of these alleles share at least one common defect. Even when expressed at high copy, we

Figure 2 (cont.) for bipolar budding), or distributed randomly. (C) Chitin deposition in V36A and V36T mutants. Haploid DLY1 (WT), DLY3497 (V36A), and DLY3553 (V36T) strains were grown to exponential phase in YEPD at 30°C, and stained with calcofluor to visualize chitin deposition. Bar, 5 μm. Apparent size differences between cells stained for chitin (unfixed), actin (fixed with ethanol), or septins (fixed with formaldehyde) are due to cell shrinkage during fixation.

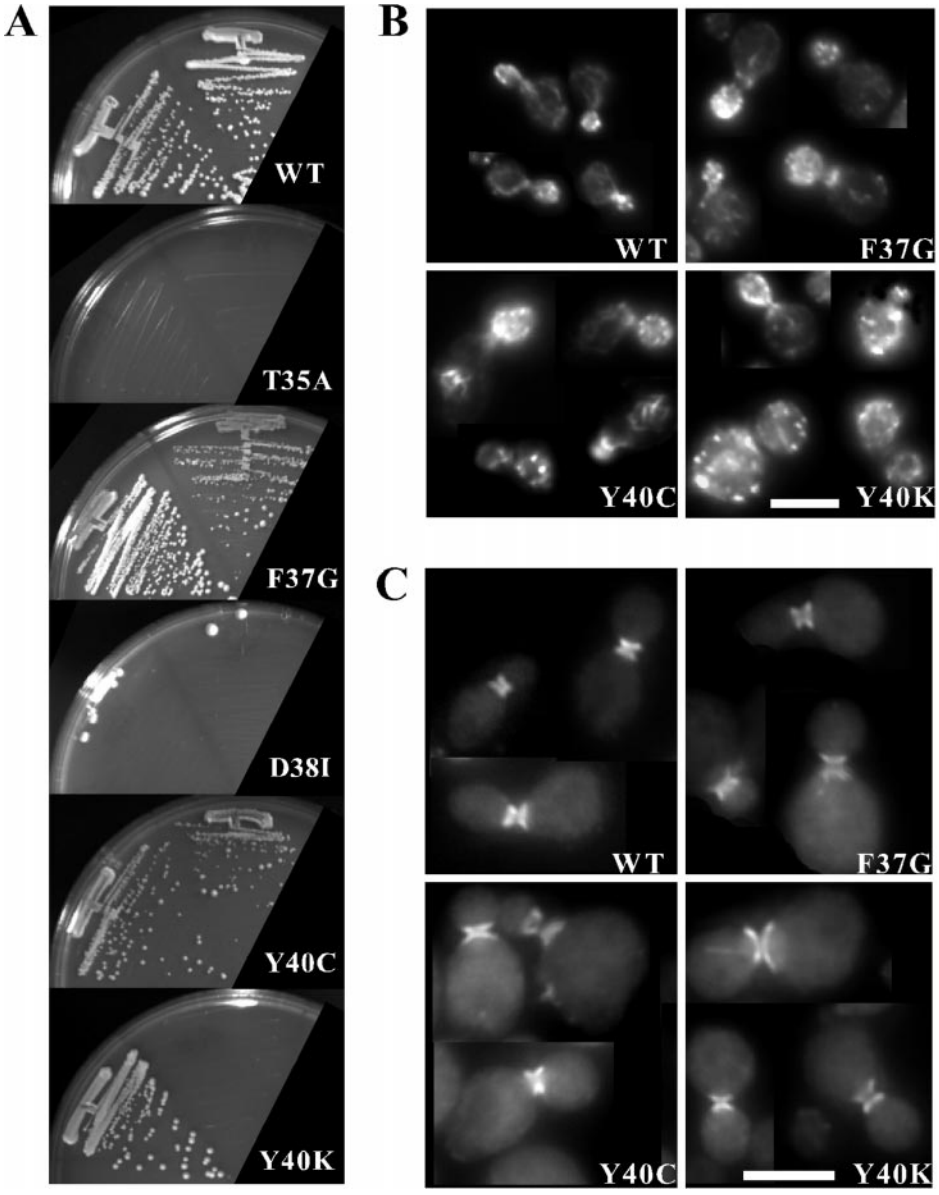

Figure 3. Effect of increased gene dosage on *cdc42* effector-loop mutant phenotype. (A) Strain DLY3067 (*GAL1p-CDC42*) was transformed with low-copy plasmids pMOSB55 (WT), pMOSB186 (T35A), pMOSB40 (F37G), pDLB1323 (D38I), pMOSB176 (Y40C), and pMOSB41 (Y40K), or with high-copy plasmids pDLB1666 (WT), pDLB1656 (T35A), pDLB1659 (F37G), pDLB1662 (D38I), pDLB1664 (Y40C), and pDLB1665 (Y40K). Cells were depleted of *GAL1*-regulated wild-type Cdc42p by growth on dextrose-containing medium for 30 h, streaked out on dextrose plates lacking uracil and incubated for 72 h at 30°C. Left streaks have high-copy plasmid and right streaks have low-copy plasmid. Actin (B) and septin (C) staining of cells containing the indicated high-copy plasmids grown as described above.

failed to detect a significant improvement in the phenotype of cells containing pairs of these alleles compared with cells containing the milder allele on its own (our unpublished results). Thus, even the apparently more specific phenotypes exhibited by cells containing high-copy *cdc42*^{F37G}, *cdc42*^{Y40C}, or *cdc42*^{Y40K} plasmids do not seem to arise from defects in cleanly separable pathways.

Strikingly, we found that *cdc42*^{V36A}/*cdc42*^{Y40C}, *cdc42*^{V36T}/*cdc42*^{Y40C}, *cdc42*^{V36A}/*cdc42*^{Y40K}, and *cdc42*^{V36T}/*cdc42*^{Y40K} heterozygotes appeared fully wild type with respect to growth, cell and mother-bud neck morphology, actin organization, and septin organization (Figure 4; our unpublished results). Thus, even though *cdc42*^{Y40C} and *cdc42*^{Y40K} were unable to promote septin organization on their own at single copy (Figure 2A), they apparently retained the ability to activate the effector pathway(s) impaired in the *cdc42*^{V36A} and *cdc42*^{V36T} mutants. In contrast, *cdc42*^{F37G} did not complement these defects when present at single copy, and only mildly ameliorated the *cdc42*^{V36T} neck defect when present at high copy, promoting slightly more narrow but still abnormal necks. *cdc42*^{T35A}, *cdc42*^{D38I}, and *cdc42*^{D38A} were unable to rescue the neck defect of *cdc42*^{V36A} and *cdc42*^{V36T} mutants even when present at high copy (our unpublished results).

Binding of Cdc42p Variants Encoded by Effector-Loop Alleles to Putative Effectors

There are five genes in the yeast genome encoding proteins that contain a CRIB domain and are presumed to be Cdc42p effectors. CRIB domains also bind to Rac-family proteins (Burbelo *et al.*, 1995) but yeast does not contain a Rac representative, so it seems likely that in yeast Cdc42p is the sole

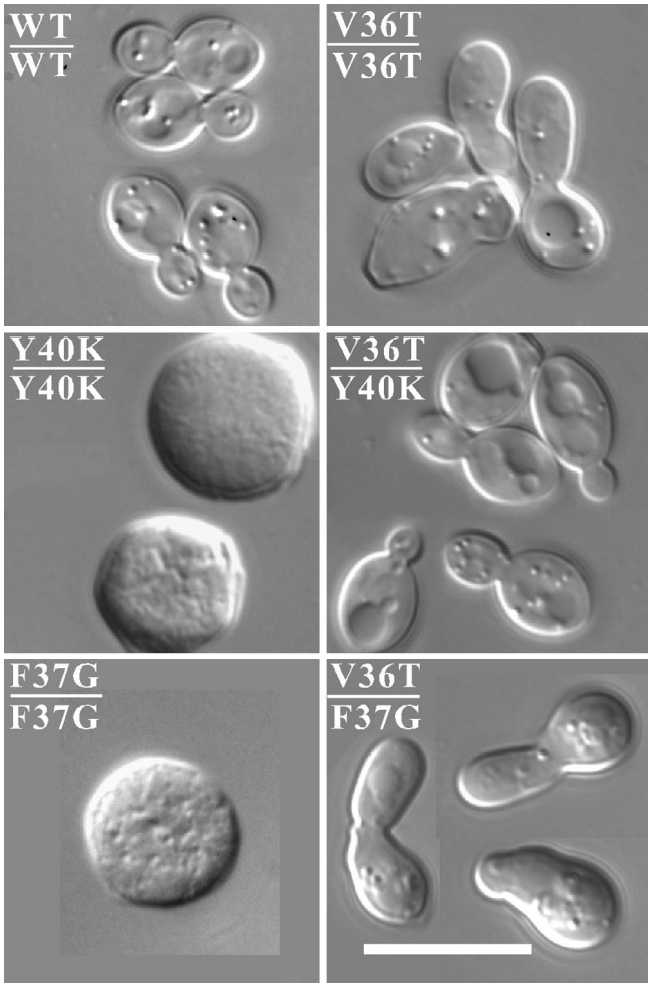

Figure 4. Intragenic complementation between *cdc42*^{Y40K} and *cdc42*^{V36T}. Cell morphology of diploid strains DLY5 (WT/WT), DLY3924 (V36T/V36T), DLY3572 (Y40K/Y40K), DLY3895 (V36T/Y40K), DLY3571 (F37G/F37G), and DLY3891 (V36T/F37G) grown in YEPD at 30°C for at least 36 h. Bar, 5 μm.

small GTPase that binds to this domain. Three of the effectors are p21-activated kinases (Cla4p, Ste20p, and Skm1p) (Leberer *et al.*, 1992; Cvrckova *et al.*, 1995; Martin *et al.*, 1997) and the other two (Gic1p and Gic2p) are homologous proteins that do not possess obvious enzymatic activity (Brown *et al.*, 1997; Chen *et al.*, 1997). Cla4p is required for normal septin organization (Longtine *et al.*, 2000) and shares an essential function in cell polarization with Ste20p (Cvrckova *et al.*, 1995; Holly and Blumer, 1999). Ste20p also plays a specific role in the pheromone response and pseudohyphal differentiation pathways (Leberer *et al.*, 1992, 1997; Peter *et al.*, 1996), whereas Skm1p does not appear to play a major role in any of the pathways yet examined (Martin *et al.*, 1997). Gic1p and Gic2p share an important (though not essential) role in cell polarization, particularly at elevated temperatures (Brown *et al.*, 1997; Chen *et al.*, 1997; Bi *et al.*, 2000). The scaffold protein Bem1p is also important for polarization (Bender and Pringle, 1991), and binds directly to GTP-Cdc42p (but not GDP-Cdc42p [Bose *et al.*, 2001]), raising the possibility that it also acts as an effector. Although several other proteins have been implicated as possible Cdc42p effectors in yeast (Evangelista *et al.*, 1997; Bi *et al.*, 2000), direct binding to Cdc42p has yet to be demonstrated.

To ask whether the Cdc42p effector-loop variants were defective in binding to the known Cdc42p effectors, we assayed the ability of bacterially expressed Cdc42p variants to interact with bacterially expressed effector CRIB domains or to full-length Bem1p (see MATERIALS AND METHODS). With one exception, the variants showed binding defects whose severity was correlated with the severity of the phenotypic defect (Figure 5 and Table 5). The pseudo wild-type Cdc42p^{F37Y} and Cdc42p^{N39A} bound as well as the wild type to all of the effectors tested. All of the other variants displayed binding deficits that were not limited to a single effector. The variants displaying neck organization defects, Cdc42p^{V36A} and Cdc42p^{V36T}, were severely impaired in binding to Cla4p and mildly impaired in binding to Bem1p, Gic1p, Gic2p, and Ste20p (in all cases the binding defect, like the phenotypic defect, was a little more severe for Cdc42p^{V36T} than Cdc42p^{V36A}). Surprisingly, Cdc42p^{F37G}, which at single copy was unable to promote either actin polarization or septin organization, displayed a similar profile of binding defects, being slightly more impaired in binding to Cla4p but less defective in binding to Ste20p and Gic2p. The fact that Cdc42p^{F37G} displayed generally milder binding defects but much stronger phenotypic defects than Cdc42p^{V36T} suggests that other important effectors exist whose binding is more affected by Cdc42p^{F37G} than by Cdc42p^{V36T}.

Cdc42p^{Y40C} was severely impaired in binding to Cla4p, Ste20p, and Gic2p, but only mildly impaired in binding to Gic1p and Bem1p, whereas Cdc42p^{Y40K}, which displayed similar but more severe phenotypic defects, was severely impaired in binding to all effectors. Cdc42p^{D38A} was severely impaired for binding to all effectors except Ste20p. Cdc42p^{T35A} and Cdc42p^{D38I} did not exhibit detectable binding to any of the tested effectors, consistent with their behavior as null alleles in all of the genetic analyses. The finding that Cdc42p^{Y40K} displayed across-the-board binding defects (Figure 5 and Table 1) was unexpected because the intragenic complementation results (Figure 4) had suggested that Cdc42p^{Y40K} could activate effector pathways that were not engaged by Cdc42p^{V36T}.

Suppression of Effector-Loop cdc42 *Mutants by Overexpression of Effectors*

If the phenotypic defect of a *cdc42* mutant results from impaired binding to a particular effector, then increasing the abundance of that effector might suppress the phenotype. To determine whether this was the case for any of the effector-loop mutants, we transformed high-copy plasmids expressing *CLA4*, *STE20*, *GIC1*, *GIC2*, *BEM1*, or *BNI1* (a formin-homology protein that has been implicated as a possible Cdc42p effector for cell polarization during mating [Evangelista *et al.*, 1997]) into mutant strains expressing the severe *cdc42* mutants on low-copy plasmids (Table 6 and Figure 6A), or the mild *cdc42* mutants at single copy (Figure 6B; data not shown). Strikingly, we found that overexpression of Cla4p was able to partially suppress the growth defect of all of the alleles except the apparently null *cdc42*^{T35A}. Similarly,

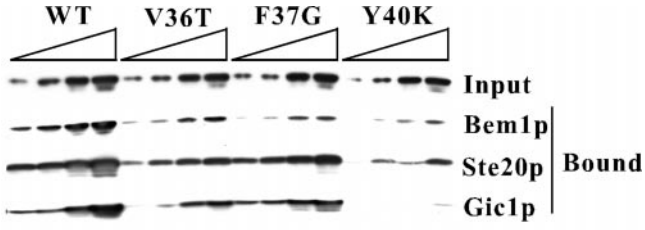

Figure 5. Binding of Cdc42p variants encoded by effector-loop mutants to known Cdc42p effectors. Plasmids pDLB1305 (Bem1p), pMOSB240 (Ste20p), pDLB1127 (Gic1p), pDLB1238 (WT), pDLB1241 (V36T), pDLB1282 (F37G), or pDLB1243 (Y40K) were used to express recombinant GST-tagged effector domains or myc-tagged Cdc42p variants in bacteria. Increasing amounts (twofold increases going from left to right) of lysates containing the myc-tagged Cdc42p variants ("input", top) were incubated with constant (excess) amounts of the indicated GST-effectors immobilized on beads, and the amount of myc-Cdc42p remaining bound after washing was determined by immunoblotting.

overexpression of Bem1p could partially suppress the growth defect of all of the alleles except *cdc42*^{T35A} and *cdc42*^{D38I} (Table 6). Suppression was not complete, because even the cells from strains exhibiting robust growth still displayed significant actin patch depolarization and morphological abnormalities (Figure 6A; data not shown). In addition, overexpression of either Cla4p or Bem1p effectively suppressed the neck morphology and septin organization defects of the *cdc42*^{V36A} and *cdc42*^{V36T} mutants (Figure 6B; data not shown).

In contrast to the general suppression conferred by Cla4p and Bem1p, other effectors were more restricted and less effective in their actions. Overexpression of Gic1p, Gic2p, or Ste20p weakly suppressed the growth defect of *cdc42*^{Y40C} mutants, whereas overexpression of Ste20p weakly suppressed the growth defect of *cdc42*^{F37G} mutants (Table 6). We did not observe suppression of any other *cdc42* mutant by these effectors, and none of the mutants was suppressed by overexpressed Bni1p or Cdc24p (Table 6).

Table 5. Binding of Cdc42p variants to recombinant effector domains[a]

	Ste20p	Cla4p	Gic1p	Gic2p	Bem1p
WT[b]	++	++	++	++	++
D57Y	−	−	−	−	−
T35A[b]	−	−	−	−	−
V36A[b]	+	+/−	+	+	+
V36T[b]	+	+/−	+	+	+
F37G[b]	++	−	+	++	+
F37Y[b]	++	++	++	++	++
D38A[b]	+	−	+/−	+/−	+/−
D38I[b]	−	−	−	−	−
N39A[b]	++	++	++	++	++
Y40C[b]	+/−	+/−	+	+/−	+
Y40K[b]	+/−	−	−	−	+/−

[a] Binding was evaluated as >70% of wild-type (++), 30–70% of wild-type (+), <30% of wild-type (+/−), or undetectable (−).

[b] All recombinant Cdc42p proteins, except D57Y, had Q61L substitutions to prevent GTP hydrolysis.

DISCUSSION

Comparison with Other Studies of Effector-Loop Mutants of Small GTPases

Previous studies conducted using effector-loop mutants in mammalian GTPases have examined the effects of the mutations on the dramatic and sometimes lethal phenotypes (e.g., oncogenic transformation or cytoskeletal derangement) induced upon overexpression of GTP-locked forms of the GTPases. Phenotypic differences in the mutants were then correlated with biochemical defects in binding to recombinant effectors in vitro, helping to elucidate the signaling pathways involved. Our strategy for characterizing the *cdc42* effector-loop mutants in yeast sought to combine the advantages of this approach with the genetic tractability of the yeast system. In particular, we characterized mutant phenotypes in the context of non-GTP-locked variants, and examined recessive defects by replacing the endogenous wild-type *CDC42* with the mutant alleles. One surprising result of this analysis was that several of the mutants displayed an essentially null phenotype rather than the expected specific defect in one or two pathways. In at least one case (*cdc42*^{Y40C}), the very same allele of mammalian *CDC42* had been reported to display specific defects in p21-activated kinase activation while retaining the ability to alter cytoskeletal behavior and promote cell cycle progression (Lamarche *et al.*, 1996). It is possible that different effectors mediate cytoskeletal control pathways in yeast and mammalian cells, because many of the putative Cdc42p effectors identified in mammals (Van Aelst and D'Souza-Schorey, 1997) have no clear homologues in yeast, where only CRIB-domain containing proteins have been clearly established as Cdc42p effectors. However, another factor likely to contribute to the difference is the level of expression of the mutant forms of Cdc42p. We found that for several alleles, elevated expression suppressed the phenotypic defect; for instance, *cdc42*^{Y40C} was able to sustain proliferation, to polarize actin (albeit imperfectly), and to organize septins when expressed at higher levels. This finding suggests that the defects due to effector-loop mutants may be less specific than previously appreciated, and that overexpression studies may reveal only the most critically affected pathways.

While this work was in progress, an overlapping set of *cdc42* mutants was generated by Kozminski *et al.* (2000). That study is complementary to ours in that we report more in-depth analysis of mutant phenotypes and effector interactions, whereas they report a considerably broader spectrum of mutants, the majority of which lie outside of the effector loop. The two studies are in agreement on the lethality of several mutants when expressed at single copy, but report some differences in the phenotype of the milder *cdc42*^{V36T} allele (discussed in more detail below), which are likely due to strain background differences. Very recently, Richman and Johnson (2000) also reported the generation of effector-loop mutants of *CDC42* in yeast, focused on characterization of a novel mutant, *cdc42*^{D38E}, that produced a phenotype distinct from any of the mutants reported here. Specifically, that mutant had an apparent defect in maintaining polarization during bud growth, leading to the frequent abandonment of small buds followed by repolarization toward new sites (Richman and Johnson, 2000). The availability of a much wider range of *cdc42* mutants should accelerate

Table 6. Suppression of *cdc42* mutant growth defect by overexpressed effectors[a]

	STE20	*CLA4*	*GIC1*	*GIC2*	*BEM1*	*BNI1*	*CDC24*	*vector*
T35A	−	−	−	−	−	−	−	−
F37G	+	++	+/−	+/−	++	+/−	+/−	+/−
D38A	−	+	−	−	+	−	−	−
D38I	−	+/−	−	−	−	−	−	−
Y40C	+	++	+	++	++	+/−	+/−	+/−
Y40K	−	+	−	−	+	−	−	−

aDLY3067 was transformed with the low-copy pMOSB46 (T35A), pMOSB48 (F37G), pMOSB49 D38I), pMOSB50 (D38A), pMOSB51 (Y40K), and pMOSB175 (Y40C) plasmids, and then with the high-copy pDLB678 (*BEM1*), pDLB722 (*CLA4*), pDLB723 (*STE20*), pDLB935 (*CDC24*), pDLB1308 *BNI1*), pMOSB229 (*GIC1*), pMOSB230 (*GIC2*), or YEp 24 (*vector*) plasmids. Growth on dextrose medium was classified as robust (++), slow (+), very poor (+/−), or none (−).

progress in understanding the pathways whereby Cdc42p controls cell polarity in yeast. Finally, using a random mutagenesis approach to investigate the role of Cdc42p in the pheromone-stimulated signal transduction pathway, we recently identified effector-loop mutations implicating Ste20p and Bem1p as the relevant effectors of Cdc42p in that pathway (Moskow *et al.*, 2000).

Phenotypes of cdc42 *Effector-Loop Mutants*

When expressed at elevated levels, *cdc42*^{Y40C} and *cdc42*^{Y40K} were able to sustain proliferation, but displayed considerably reduced polarization of actin patches (more severe for *cdc42*^{Y40K} than *cdc42*^{Y40C}) and frequent generation of multinucleate cells (more severe for *cdc42*^{Y40C} than *cdc42*^{Y40K}). These phenotypes are reminiscent of those in null mutants lacking the polarity establishment proteins Bem1p or Bem2p (Bender and Pringle, 1991; Pringle *et al.*, 1995), and may indicate a severe defect in promoting proper actin polarization. Interpretation of a "depolarized actin patch" phenotype is complicated by the recent finding that actin patch depolarization is induced by plasma membrane or cell wall stress-signaling pathways involving Pkc1p (Delley and Hall, 1999). However, the proportion of cells with depolarized patches was only reduced by 20–30% when these strains were grown in osmotically stabilized media (containing 1 M sorbitol, which suppresses cell wall defects and Pkc1p pathway activation [Kamada *et al.*, 1995]), suggesting that most of the patch delocalization is due to a primary defect in actin organization (our unpublished results).

In addition to actin patch depolarization, *cdc42*^{Y40C} mutant cells frequently contained actin "ropes," thicker than normal cables and generally forming knotted clumps within the mother portion of budded cells. Because these structures were observed using phalloidin, we assume that they consist of polymerized actin and most likely represent aberrant cables. Because actin cables play a role in spindle orientation and nuclear segregation (Theesfeld *et al.*, 1999), these aberrant cables may contribute to the increased frequency of binucleate and multinucleate cells in the *cdc42*^{Y40C} population. This is a novel *cdc42* phenotype that may indicate a role for Cdc42p in regulating the cross-linking or assembly dynamics of actin cables.

Two other alleles, *cdc42*^{V36A} and *cdc42*^{V36T}, were able to sustain proliferation even when expressed at single copy, but displayed aberrant morphology of the mother-bud neck accompanied by defects in septin localization and associated defects in chitin deposition and bud site selection (more severe for *cdc42*^{V36T} than *cdc42*^{V36A}). These phenotypes suggest a primary defect in septin organization, although they do not exclude the possibility (previously suggested for *ste20*Δ *cla4-Ts* mutants [Cvrckova *et al.*, 1995]) that a primary defect in some other aspect of neck organization produces secondary effects on septin localization and function.

The *cdc42*^{V36T} mutant was also analyzed by Kozminski *et al.* (2000), who did not examine septin localization or mention neck morphology but did report that the mutants exhibited elongated buds and hyperpolarized actin patches. They concluded that this mutant had a primary defect in the switch from apical-to-isotropic growth, which is associated with a depolarization of actin patches within the bud (Kozminski *et al.*, 2000). However, examination of the *cdc42*^{V36T} cells in that report suggests that they also have defects in neck morphology similar to those observed in our strain background. Furthermore, recent studies (Barral *et al.*, 1999; Longtine *et al.*, 2000) indicate that defects in septin organization frequently trigger a Swe1p-dependent G2 delay that delays the apical-isotropic switch and leads to bud elongation, raising the possibility that the bud elongation observed by Kozminski *et al.* (2000) was a secondary consequence of altered septin organization. In this context, it is noteworthy that another mutant, *cdc42*^{V44A}, was recently reported to show both septin organization defects and elongated buds, and in that case the bud elongation was shown to be Swe1p-dependent (Richman *et al.*, 1999). We did not observe significant bud elongation in *cdc42*^{V36T} cells in our strain background, but previous observations suggest that mutants causing increased Swe1p activity (e.g., *hsl1*Δ or *hsl7*Δ mutants [McMillan *et al.*, 1999]) display much weaker elongated-bud phenotypes in this strain background. Thus, we suggest that the primary defect in *cdc42*^{V36T} mutants lies in a pathway important for septin or neck organization, which in some strain backgrounds gives rise to a secondary Swe1p-dependent bud elongation.

Biochemical analysis indicated that *cdc42*^{V36T} mutants were defective in binding to the Cla4p CRIB domain, and *cla4*Δ mutants display defects in septin organization (Cvrckova *et al.*, 1995; Longtine *et al.*, 2000), raising the possibility that the neck defects of this mutant are due to impairment of Cla4p function. However, other mutants (*cdc42*^{Y40C} and *cdc42*^{Y40K}) that also failed to bind to the Cla4p CRIB domain were nevertheless effective in complementing the *cdc42*^{V36T} defect. It remains unclear whether the Cdc42p–Cla4p interaction is important for

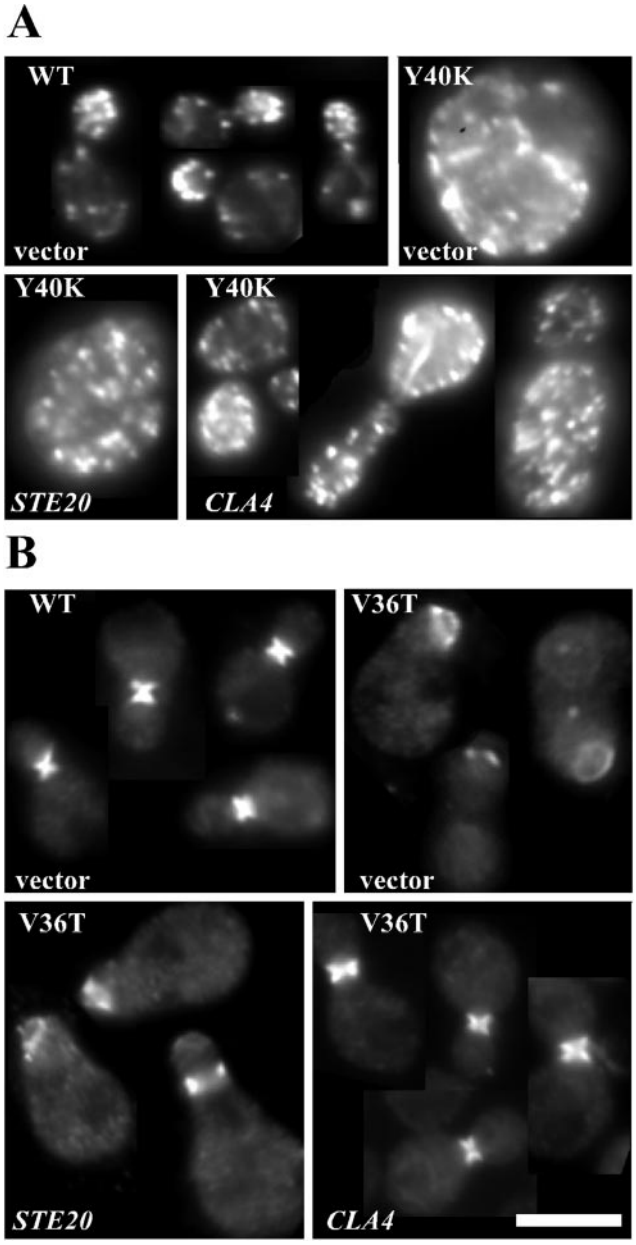

Figure 6. Suppression of *cdc42* effector-loop mutants by overexpression of *CLA4*. DLY1 (WT), DLY3513 (Y40K), and DLY3500 (V36T) strains were transformed with high-copy plasmids YEp24 (vector), pDLB722 (*CLA4*), or pDLB723 (*STE20*) as indicated and grown in dextrose medium lacking uracil at 30°C. (A) Cells were stained with rhodamine-phalloidin to visualize F-actin. (B) Cells were stained with anti-Cdc11p antibody to visualize septins. Bar, 5 μm.

the role of Cla4p in septin organization, and if so whether defects in a Cla4p-mediated pathway are important for the *cdc42*^{V36T} phenotype.

Evidence for Existence of Further Cdc42p Effectors

By the criterion of functional complementation, the *cdc42*^{V36A} and *cdc42*^{V36T} mutants are defective in separate pathways from those that are defective in *cdc42*^{Y40C} and *cdc42*^{Y40K} mutants. It was particularly surprising to find that *cdc42*^{V36T}/*cdc42*^{Y40K} diploids appeared fully wild type, for two reasons. First, homozygous diploid cells containing two copies of *cdc42*^{Y40K} were unable to polarize actin or assemble septins and arrested with a characteristic *cdc42* null phenotype, yet even at single copy (i.e. one of the two copies in the heterozygote) *cdc42*^{Y40K} was able to correct the neck defect of *cdc42*^{V36T} mutants. Second, whereas Cdc42p^{V36T} retained the ability to interact with most of the effectors we tested (Ste20p, Gic1p, Gic2p, Bem1p) at a level only mildly reduced from the wild type, interaction between the effectors and Cdc42p^{Y40K} was significantly more impaired in every case. This suggests that none of these effectors is responsible for the complementing activity of Cdc42p^{Y40K}, and therefore that a novel effector(s) important for septin or neck organization exists.

The *cdc42*^{F37G} mutant, at single copy, was also unable to polarize actin or assemble septins and arrested with a characteristic *cdc42* null phenotype. However, with the possible exception of Cla4p, Cdc42p^{F37G} bound at least as well to all tested effectors as did Cdc42p^{V36T}. This suggests that none of these effectors accounts for the lethal phenotypic defect of the *cdc42*^{F37G} mutant, and therefore that a novel effector(s) important for actin polarization and bud formation exists. However, it is also possible that in vitro binding does not accurately reflect productive in vivo interaction. For instance, it may be that interaction of Cdc42p^{F37G} with Ste20p fails to activate Ste20p kinase activity, whereas interaction of Cdc42p^{V36T} with Ste20p, although reduced, can activate Ste20p kinase activity. In that case, the more severe phenotype of *cdc42*^{F37G} mutants might reflect the reduced productivity of its interactions with known effectors rather than its inability to interact with other (hypothetical) effectors.

Role of Cla4p and Bem1p in Cell Polarity

One remarkable result to emerge from this work is that overexpression of Cla4p or Bem1p was able to partially suppress the phenotypic defects of almost every single effector-loop mutant (with the notable exception of *cdc42*^{T35A}, which is thought to prevent all effector binding). This is particularly striking because the different alleles affected genetically separable pathways (as discussed above) and displayed distinct phenotypes and effector-binding profiles. In the Kozminski *et al.* (2000) study Cla4p overexpression did not globally suppress temperature-sensitive growth defects of several mutants, and Bem1p overexpression was not tested. Conceivably, our mutants encompass a special set of alleles that is particularly susceptible to suppression by Cla4p, whereas those investigated by Kozminski *et al.* (2000) are not. However, the effectiveness of suppression may well depend upon the level of Cla4p expression, and both we (our unpublished results) and Kozminski *et al.* (2000) have found that excessive Cla4p expression is highly deleterious even in otherwise wild-type cells. This raises the possibility that the stronger expression (driven by the *GAL1/10* promoter) used by Kozminski *et al.* (2000) may have masked suppression of their mutants.

It seems very unlikely that overexpression of Cla4p or Bem1p is simply restoring adequate levels of Cla4p- or Bem1p interaction to our panel of mutants, because the differences between the mutants appear to preclude interpretation of their

defects as being due to the same downstream pathways in every case. It seems more likely that these are instances of "bypass suppression," i.e., that excess Cla4p or Bem1p can cover for loss of particular Cdc42p-directed pathways by stimulating parallel pathways. However, these parallel pathways would still have to correct several separate defects in the various mutants.

An alternative interpretation of the suppression results is that rather than acting solely downstream of Cdc42p or in parallel with Cdc42p, Cla4p and Bem1p can also act effectively "upstream" of Cdc42p (or at the same level, improving overall Cdc42p function). In this scenario, Cla4p and Bem1p may help to increase the activity of the Cdc42p effector-loop variants, yielding a phenotypic improvement similar to (but more potent than) that observed when the alleles were expressed from high-copy plasmids. Support for this hypothesis comes from recent observations that the scaffold protein Bem1p can bind directly to Cla4p, as well as to GTP-Cdc42p and to the exchange factor Cdc24p, in a complex (Bose *et al.*, 2001). Such a complex may assist Cdc24p function and/or localization, thereby increasing GTP-loading and/or localization of Cdc42p in vivo.

In conclusion, our analysis of effector-loop mutants of *CDC42* in yeast has identified partial function alleles displaying some novel *cdc42* phenotypes, and has revealed a surprisingly broad role for Bem1p and Cla4p in promoting Cdc42p function. Furthermore, the data suggest that unknown effectors involved in actin and septin organization exist, and the mutants provide a starting point for genetic approaches to identify those effectors.

ACKNOWLEDGMENTS

We thank Alan Bender, Erfei Bi, Mark Longtine, and Matthias Peter for plasmids, and Keith Kozminsky, David Drubin, and Pat Brennwald for kindly providing anti-Cdc42p antibodies. Thanks also to John Pringle and members of the Lew lab for stimulating interactions. J.J.M. was supported by American Cancer Society fellowship PF-98-008-01-CSM. This work was supported by National Institutes of Health Grant GM-53050 and American Cancer Society Grant RPG-98-046-CCG to D.J.L.

REFERENCES

Adams, A.E.M., Johnson, D.I., Longnecker, R.M., Sloat, B.F., and Pringle, J.R. (1990). *CDC42* and *CDC43*, two additional genes involved in budding and the establishment of cell polarity in the yeast *Saccharomyces cerevisiae*. J. Cell Biol. *111*, 131–142.

Adams, A.E.M., and Pringle, J.R. (1984). Relationship of actin and tubulin distribution to bud growth in wild-type and morphogenetic-mutant *Saccharomyces cerevisiae*. J. Cell Biol. *98*, 934–945.

Ausubel, F.M., Brent, R., Kingston, R.E., Moore, D.D., Seidman, J.G., Smith, J.A., and Struhl, K. (1995). Current Protocols in Molecular Biology, New York: John Wiley & Sons.

Ayscough, K.R., Stryker, J., Pokala, N., Sanders, M., Crews, P., and Drubin, D.G. (1997). High rates of actin filament turnover in budding yeast and roles for actin in establishment and maintenance of cell polarity revealed using the actin inhibitor latrunculin-A. J. Cell Biol. *137*, 399–416.

Barral, Y., Parra, M., Bidlingmaier, S., and Snyder, M. (1999). Nim1-related kinases coordinate cell cycle progression with the organization of the peripheral cytoskeleton in yeast. Genes Dev. *13*, 176–187.

Bender, A., and Pringle, J.R. (1991). Use of a screen for synthetic lethal and multicopy suppressee mutants to identify two new genes involved in morphogenesis in *Saccharomyces cerevisiae*. Mol. Cell. Biol. *11*, 1295–1305.

Bi, E., Chiavetta, J.B., Chen, H., Chen, G.C., Chan, C.S., and Pringle, J.R. (2000). Identification of novel, evolutionarily conserved Cdc42p-interacting proteins and of redundant pathways linking Cdc24p and Cdc42p to actin polarization in yeast. Mol. Biol. Cell. *11*, 773–793.

Bi, E., Maddox, P., Lew, D.J., Salmon, E.D., McMillan, J.N., Yeh, E., and Pringle, J.R. (1998). Involvement of an actomyosin contractile ring in *Saccharomyces cerevisiae* cytokinesis. J. Cell Biol. *142*, 1301–1312.

Bi, E., and Zigmond, S.H. (1999). Actin polymerization: where the WASP stings. Curr. Biol. *9*, R160–R163.

Bose, I., Irazoqui, J., Moskow, J.J., Bardes, E.S.G., Zyla, T.R., and Lew, D.J. (2001). Assembly of scaffold-mediated complexes containing Cdc42p, the exchange factor Cdc24p, and the effector Cla4p required for cell cycle regulated phosphorylation of Cdc24p. J. Biol. Chem. (*in press*).

Brown, J.L., Jaquenoud, M., Gulli, M.P., Chant, J., and Peter, M. (1997). Novel Cdc42-binding proteins Gic1 and Gic2 control cell polarity in yeast. Genes Dev. *11*, 2972–2982.

Brown, A.M., O'Sullivan, A.J., and Gomperts, B.D. (1998). Induction of exocytosis from permeabilized mast cells by the guanosine triphosphatases Rac and Cdc42. Mol. Biol. Cell *9*, 1053–1063.

Burbelo, P.D., Drechsel, D., and Hall, A. (1995). A conserved binding motif defines numerous candidate target proteins for both Cdc42 and Rac GTPases. J. Biol. Chem. *270*, 29071–29074.

Chen, G.C., Kim, Y.J., and Chan, C.S. (1997). The Cdc42 GTPase-associated proteins Gic1 and Gic2 are required for polarized cell growth in *Saccharomyces cerevisiae*. Genes Dev. *11*, 2958–2971.

Christianson, T.W., Sikorski, R.S., Dante, M., Shero, J.H., and Hieter, P. (1992). Multifunctional yeast high-copy-number shuttle vectors. Gene *110*, 119–122.

Coso, O.A., Chiariello, M., Yu, J.-C., Teramoto, H., Crespo, P., Xu, N., Miki, T., and Gutkind, J.S. (1995). The small GTP-binding proteins Rac1 and Cdc42 regulate the activity of the JNK/SAPK signaling pathway. Cell *81*, 1137–1146.

Cvrckova, F., De Virgilio, C., Manser, E., Pringle, J.R., and Nasmyth, K. (1995). Ste20-like protein kinases are required for normal localization of cell growth and for cytokinesis in budding yeast. Genes Dev. *9*, 1817–1830.

Delley, P.A., and Hall, M.N. (1999). Cell wall stress depolarizes cell growth via hyperactivation of RHO1. J. Cell Biol. *147*, 163–174.

Diekmann, D., Nobes, C.D., Burbelo, P.D., Abo, A., and Hall, A. (1995). Rac GTPase interacts with GAPs and target proteins through multiple effector sites. EMBO J. *14*, 5297–5305.

Evangelista, M., Blundell, K., Longtine, M.S., Chow, C.J., Adames, N., Pringle, J.R., Peter, M., and Boone, C. (1997). Bni1p, a yeast formin linking Cdc42p and the actin cytoskeleton during polarized morphogenesis. Science *276*, 118–122.

Flescher, E.G., Madden, K., and Snyder, M. (1993). Components required for cytokinesis are important for bud site selection in yeast. J. Cell Biol. *122*, 373–386.

Garrett, W.S., Chen, L.M., Kroschewski, R., Ebersold, M., Turley, S., Trombetta, S., Galan, J.E., and Mellman, I. (2000). Developmental control of endocytosis in dendritic cells by Cdc42. Cell *102*, 325–334.

Guthrie, C., and Fink, G.R. (1991). Guide to Yeast Genetics and Molecular Biology.

Hall, A. (1998). Rho GTPases and the actin cytoskeleton. Science *279*, 509–514.

Holly, S.P., and Blumer, K.J. (1999). PAK-family kinases regulate cell and actin polarization throughout the cell cycle of *Saccharomyces cerevisiae*. J. Cell Biol. *147*, 845–856.

Jaquenoud, M., Gulli, M.P., Peter, K., and Peter, M. (1998). The Cdc42p effector Gic2p is targeted for ubiquitin-dependent degradation by the SCFGrr1 complex. EMBO J. *17*, 5360–5373.

Johnson, D.I. (1999). Cdc42: an essential Rho-type GTPase controlling eukaryotic cell polarity. Microbiol. Mol. Biol. Rev. *63*, 54–105.

Joneson, T., and Bar-Sagi, D. (1997). Ras effectors and their role in mitogenesis and oncogenesis. J. Mol. Med. *75*, 587–593.

Joneson, T., McDonough, M., Bar-Sagi, D., and Van Aelst, L. (1996a). RAC regulation of actin polymerization and proliferation by a pathway distinct from Jun kinase. Science *274*, 1374–1376.

Joneson, T., White, M.A., Wigler, M.H., and Bar-Sagi, D. (1996b). Stimulation of membrane ruffling and MAP kinase activation by distinct effectors of RAS. Science *271*, 810–812.

Kamada, Y., Jung, U.S., Piotrowski, J., and Levin, D.E. (1995). The protein kinase C-activated MAP kinase pathway of *Saccharomyces cerevisiae* mediates a novel aspect of the heat shock response. Genes Dev. *9*, 1559–1571.

Khosravi-Far, R., White, M.A., Westwick, J.K., Solski, P.A., Chrzanowska-Wodnicka, M., Van Aelst, L., Wigler, M.H., and Der, C.J. (1996). Oncogenic Ras activation of Raf/mitogen-activated protein kinase-independent pathways is sufficient to cause tumorigenic transformation. Mol. Cell. Biol. *16*, 3923–3933.

Kozminski, K.G., Chen, A.J., Rodal, A.A., and Drubin, D.G. (2000). Functions and functional domains of the GTPase Cdc42p. Mol. Biol. Cell *11*, 339–354.

Kroschewski, R., Hall, A., and Mellman, I. (1999). Cdc42 controls secretory and endocytic transport to the basolateral plasma membrane of MDCK cells. Nat. Cell Biol. *1*, 8–13.

Lamarche, N., Tapon, N., Stowers, L., Burbelo, P.D., Aspenstrom, P., Bridges, T., Chant, J., and Hall, A. (1996). Rac and Cdc42 induce actin polymerization and G1 cell cycle progression independently of p65PAK and the JNK/SAPK MAP kinase cascade. Cell *87*, 519–529.

Leberer, E., Dignard, D., Harcus, D., Thomas, D.Y., and Whiteway, M. (1992). The protein kinase homologue Ste20p is required to link the yeast pheromone response G-protein bg subunits to downstream signaling components. EMBO J. *11*, 4815–4824.

Leberer, E., Wu, C., Leeuw, T., Fourest-Lieuvin, A., Segall, J.E., and Thomas, D.Y. (1997). Functional characterization of the Cdc42p binding domain of yeast Ste20p protein kinase. EMBO J. *16*, 83–97.

Lehman, K., Rossi, G., Adamo, J.E., and Brennwald, P. (1999). Yeast homologues of tomosyn and lethal giant larvae function in exocytosis and are associated with the plasma membrane SNARE, Sec9. J. Cell Biol. *146*, 125–140.

Lew, D.J., and Reed, S.I. (1993). Morphogenesis in the yeast cell cycle: regulation by Cdc28 and cyclins. J. Cell Biol. *120*, 1305–1320.

Li, R., Zheng, Y., and Drubin, D.G. (1995). Regulation of cortical actin cytoskeleton assembly during polarized cell growth in budding yeast. J. Cell Biol. *128*, 599–615.

Liu, Q., Li, M.Z., Leibham, D., Cortez, D., and Elledge, S.J. (1998). The univector plasmid-fusion system, a method for rapid construction of recombinant DNA without restriction enzymes. Curr. Biol. *8*, 1300–1309.

Longtine, M.S., Theesfeld, C.L., McMillan, J.N., Weaver, E., Pringle, J.R., and Lew, D.J. (2000). Septin-dependent assembly of a cell-cycle-regulatory module in *Saccharomyces cerevisiae*. Mol. Cell Biol. *20*, 4049–4061.

Manser, E., Leung, T., Salihuddin, H., Tan, L., and Lim, L. (1993). A non-receptor tyrosine kinase that inhibits the GTPase activity of p21 Cdc42. Nature *363*, 364–367.

Manser, E., Leung, T., Salihuddin, H., Zhao, Z., and Lim, L. (1994). A brain serine/threonine protein kinase activated by Cdc42 and Rac1. Nature *367*, 40–46.

Martin, H., Mendoza, A., Rodriguez-Pachon, J.M., Molina, M., and Nombela, C. (1997). Characterization of *SKM1*, a *Saccharomyces cerevisiae* gene encoding a novel Ste20/PAK-like protein kinase. Mol. Microbiol. *23*, 431–444.

McMillan, J.N., Longtine, M.S., Sia, R.A., Theesfeld, C.L., Bardes, E.S., Pringle, J.R., and Lew, D.J. (1999). The morphogenesis checkpoint in *Saccharomyces cerevisiae*: cell cycle control of Swe1p degradation by Hsl1p and Hsl7p. Mol. Cell. Biol. *19*, 6929–6939.

Minden, A., Lin, A., Claret, F.X., Abo, A., and Karin, M. (1995). Selective activation of the JNK signaling cascade and c-Jun transcriptional activity by the small GTPases Rac and Cdc42Hs. Cell *81*, 1147–1157.

Moskow, J.J., Gladfelter, A.S., Lamson, R.E., Pryciak, P.M., and Lew, D.J. (2000). Role of Cdc42p in pheromone-stimulated signal transduction in *Saccharomyces cerevisiae*. Mol. Cell. Biol. *20*, 7559–7571.

Nobes, C.D., and Hall, A. (1995). Rho, rac, and cdc42 GTPases regulate the assembly of multimolecular focal complexes associated with actin stress fibers, lamellipodia, and filopodia. Cell *81*, 53–62.

Owen, D., Mott, H.R., Laue, E.D., and Lowe, P.N. (2000). Residues in Cdc42 that specify binding to individual CRIB effector proteins. Biochemistry *39*, 1243–1250.

Pai, E.F., Krengel, U., Petsko, G.A., Goody, R.S., Kabsch, W., and Wittinghofer, A. (1990). Refined crystal structure of the triphosphate conformation of H-ras p21 at 1.35 A resolution: implications for the mechanism of GTP hydrolysis. EMBO J. *9*, 2351–2359.

Peter, M., Neiman, A.M., Park, H.-O., van Lohuizen, M., and Herskowitz, I. (1996). Functional analysis of the interaction between the small GTP binding protein Cdc42 and the Ste20 protein kinase in yeast. EMBO J. *15*, 7046–7059.

Pirone, D.M., Fukuhara, S., Gutkind, J.S., and Burbelo, P.D. (2000). SPECs, small binding proteins for Cdc42. J. Biol. Chem. *275*, 22650–22656.

Pringle, J.R. (1991). Staining of bud scars and other cell wall chitin with Calcofluor. Methods Enzymol. *194*, 732–735.

Pringle, J.R., Bi, E., Harkins, H.A., Zahner, J.E., De Virgilio, C., Chant, J., Corrado, K., and Fares, H. (1995). Establishment of cell polarity in yeast. Cold Spring Harbor Symp. Quant. Biol. *60*, 729–744.

Redding, K., Holcomb, C., and Fuller, R.S. (1991). Immunolocalization of Kex2 protease identifies a putative late Golgi compartment in the yeast *Saccharomyces cerevisiae*. J. Cell Biol. *113*, 527–538.

Richardson, H.E., Wittenberg, C., Cross, F., and Reed, S.I. (1989). An essential G1 function for cyclin-like proteins in yeast. Cell *59*, 1127–1133.

Richman, T.J., and Johnson, D.I. (2000). *Saccharomyces cerevisiae* Cdc42p GTPase is involved in preventing the recurrence of bud emergence during the cell cycle. Mol. Cell. Biol. *20*, 8548–8559.

Richman, T.J., Sawyer, M.M., and Johnson, D.I. (1999). The Cdc42p GTPase is involved in a G2/M morphogenetic checkpoint regulating the apical-isotropic switch and nuclear division in yeast. J. Biol. Chem. *274*, 16861–16870.

Rohatgi, R., Ma, L., Miki, H., Lopez, M., Kirchhausen, T., Takenawa, T., and Kirschner, M.W. (1999). The interaction between N-WASP and the Arp2/3 complex links Cdc42- dependent signals to actin assembly. Cell *97*, 221–231.

Sahai, E., Alberts, A.S., and Treisman, R. (1998). RhoA effector mutants reveal distinct effector pathways for cytoskeletal reorganization, SRF activation and transformation. EMBO J. *17*, 1350–1361.

Sells, M.A., Knaus, U.G., Bagrodia, S., Ambrose, D.M., Bokoch, G.M., and Chernoff, J. (1997). Human p21-activated kinase (Pak1) regulates actin organization in mammalian cells. Curr. Biol. *7*, 202–210.

Sia, R.A.L., Herald, H.A., and Lew, D.J. (1996). Cdc28 tyrosine phosphorylation and the morphogenesis checkpoint in budding yeast. Mol. Biol. Cell *7*, 1657–1666.

Sikorski, R.S., and Hieter, P. (1989). A system of shuttle vectors and yeast host strains designed for efficient manipulation of DNA in *Saccharomyces cerevisiae*. Genetics *122*, 19–27.

Simon, M.N., De Virgilio, C., Souza, B., Pringle, J.R., Abo, A., and Reed, S.I. (1995). Role for the Rho-family GTPase Cdc42 in yeast mating-pheromone signal pathway. Nature *376*, 702–705.

Theesfeld, C.L., Irazoqui, J.E., Bloom, K., and Lew, D.J. (1999). The role of actin in spindle orientation changes during the *Saccharomyces cerevisiae* cell cycle. J. Cell Biol. *146*, 1019–10132.

Van Aelst, L., and D'Souza-Schorey, C. (1997). Rho GTPases and signaling networks. Genes Dev. *11*, 2295–2322.

White, M.A., Nicolette, C., Minden, A., Polverino, A., Van Aelst, L., Karin, M., and Wigler, M.H. (1995). Multiple Ras functions can contribute to mammalian cell transformation. Cell *80*, 533–541.

White, M.A., Vale, T., Camonis, J.H., Schaefer, E., and Wigler, M.H. (1996). A role for the Ral guanine nucleotide dissociation stimulator in mediating Ras-induced transformation. J. Biol. Chem. *271*, 16439–16442.

Wittinghofer, A., and Nassar, N. (1996). How Ras-related proteins talk to their effectors. Trends Biochem. Sci. *21*, 488–491.

Yamashita, M., Yoshikuni, M., Hirai, T., Fukada, S., and Nagahama, Y. (1991). A monoclonal antibody against the PSTAIR sequence of p34cdc2, catalytic subunit of maturation-promoting factor and key regulator of the cell cycle. Develop Growth Differ. *33*, 617–624.

Yang, S., Ayscough, K.R., and Drubin, D.G. (1997). A role for the actin cytoskeleton of *Saccharomyces cerevisiae* in bipolar bud-site selection. J. Cell Biol. *136*, 111–123.

Zhao, Z.S., Leung, T., Manser, E., and Lim, L. (1995). Pheromone signaling in *Saccharomyces cerevisiae* requires the small GTP-binding protein Cdc42p and its activator Cdc24p. Mol. Cell. Biol. *15*, 5246–5257.

Zigmond, S.H., Joyce, M., Yang, C., Brown, K., Huang, M., and Pring, M. (1998). Mechanism of Cdc42-induced actin polymerization in neutrophil extracts. J. Cell Biol. *142*, 1001–1012.

Ziman, M., O'Brien, J.M., Ouellette, L.A., Church, W.R., and Johnson, D.I. (1991). Mutational analysis of *CDC42*Sc, a *Saccharomyces cerevisiae* gene that encodes a putative GTP-binding protein involved in the control of cell polarity. Mol. Cell. Biol. *11*, 3537–3544.

Ziman, M., Preuss, D., Mulholland, J., O'Brien, J.M., Botstein, D., and Johnson, D.I. (1993). Subcellular localization of Cdc42p, a *Saccharomyces cerevisiae* GTP-binding protein involved in the control of cell polarity. Mol. Biol. Cell *4*, 1307–1316.